Zootaxa 5446 (1): 001–041
https://www.mapress.com/zt/

Article

ISSN 1175-5326 (print edition)
ZOOTAXA
ISSN 1175-5334 (online edition)

https://doi.org/10.11646/zootaxa.5446.1.1
http://zoobank.org/urn:lsid:zoobank.org:pub:E0FDD64D-EA99-4AA9-A7E1-3EB074B3A0F0

The lionfishes: Comparative development of *Pterois volitans*, *Dendrochirus barberi*, and *D. hemprichi* (Scorpaeniformes: Scorpaenidae: Pteroinae) and discrimination of their early life stages from non-pteroine scorpaenid genera in the Western North Atlantic

JAMES G. DITTY[1], ESTRELLA MALCA[2,3] & LOURDES VÁSQUEZ-YEOMANS[4]
[1]*American Southwest Ichthyological Researchers (ASIR), 800 Encino Place NE, Albuquerque, New Mexico 87102–2606, USA.*
Apinchhitter@outlook.com; https://orcid.org/0000-0003-4917-3327
[2]*Cooperative Institute for Marine and Atmospheric Studies (CIMAS), University of Miami, Florida, USA.*
[3]*Southeast Fisheries Science Center, NMFS, NOAA, 75 Virginia Beach Drive, Miami, Florida 33149, USA.*
estrella.malca@noaa.gov; https://orcid.org/0000-0002-9182-5854
[4]*El Colegio de la Frontera Sur, Unidad Chetumal Av. Centenario Km 5.5, CP 77014 Chetumal, Quintana Roo, Mexico.*
lvasquez@ecosur.mx; https://orcid.org/0000-0003-2095-1404

Abstract

Despite the threat that lionfishes pose to non-native marine ecosystems worldwide, their early life stages (ELS) remain difficult to distinguish from morphologically similar taxa due to inadequate descriptions and poorly defined taxonomic characters. Two members of the Indo-Pacific marine assemblage commonly known as lionfishes, zebrafishes, firefishes, turkeyfishes, and butterfly-cods (Scorpaeniformes: Scorpaenidae: Pteroinae) are invasive in the Western North Atlantic (WNA). Here, we describe the ELS of *Pterois volitans*, *Dendrochirus barberi*, and two transforming larvae and an early juvenile of *D. hemprichi*; review the early development of *D. zebra* and a larva described as *D. bellus*; identify characteristics that distinguish *P. volitans* from the four members of *Dendrochirus*; and compile meristic and distribution data for all currently valid species of lionfishes worldwide based on recent revisions and updated nomenclature. We also briefly describe a small juvenile of two poorly known non-pteroine deep-water scorpaenids, and discuss characteristics that distinguish the five pteroines from non-pteroine scorpaenid genera in the WNA. Differences in relative length and elevation of the parietal and nuchal spines, and in pigmentation patterns distinguish *P. volitans* from the four members of *Dendrochirus*. *Pterois volitans* has parietal spines two or more times longer than the nuchals with both sets of spines oriented about 30° above the longitudinal axis of the head, whereas the four members of *Dendrochirus* have relatively short parietal and nuchal spines subequal in length that lay flatter against the cranium (i.e., elevation ≤15° above longitudinal axis of head). Transforming larvae of the four members of *Dendrochirus* also develop saddles of pigment along the dorsal and ventral margins of the body that *P. volitans* lacks at the sizes examined. One or more of the following suite of traits distinguish larvae of the five pteroines from those of non-pteroine scorpaenids and other morphologically similar taxa: the presence or absence of a "shield" of pigment over the dorsolateral margin of the visceral mass (may be reduced or augmented with scattered blotches of pigment in larger larvae of some taxa); the relative length, elevation, and placement of the parietal and nuchal spines; the presence or absence of a small slit behind the fourth gill arch; differences in pectoral-fin length, shape, and extent of pigmentation; the relative size, length, and placement of spines along the posterior shelf of the preopercle (PPO); and the presence or absence, number, and placement of spine(s) along the opercle.

Key words: *Dendrochirus zebra*; *Dendrochirus* "*bellus*"; *Phenacoscorpius nebris*; *Trachyscorpia cristulata*; larvae; zoogeography; size-at-settlement

Introduction

Native to the Indo-Pacific, the marine assemblage known as lionfishes, zebrafishes, firefishes, turkeyfishes, or butterfly-cods (Teleostei: Scorpaenidae, Pteroinae) currently consists of five genera and 29 valid species (Table 1) with nearly 25% described or re-described since 2013 (Fricke *et al*. 2023). Here, we collectively refer to all taxa as lionfishes. The lionfishes have a zebra-like, aposematic color pattern, pectoral fins with 17–18 venomous spines, and most species have numerous ornate tentacles and dermal flaps on the head and median fins.

Accepted by K. Tang: 13 Dec. 2023; published: 29 Apr. 2024

TABLE 1. Distribution of currently valid species of the Indo-Pacific lionfishes (Teleostei: Scorpaenidae, Pteroinae) based on taxonomic revisions and updated species nomenclature.

Taxon	Distribution	References
Brachypterois		
B. curvispina	Off northern & northeastern coasts of Queensland, Australia	Matsunuma *et al*. (2013); Matsunuma & Motomura (2017)
B. serrulata	Gulf of Thailand south to Borneo, north through South China Sea & Taiwan to southern Japan	Matsunuma *et al*. (2013)
B. serrulifer	Madagascar, Red Sea, Persian Gulf & Gulf of Oman through Indian Ocean & Andaman Sea, southward through Indonesia to Gulf of Carpentaria, northward through The Philippines & China Sea to southern Japan	Matsunuma *et al*. (2013); Matsunuma & Motomura (2017)
Dendrochirus		
D. barberi	Endemic to Hawai'ian Islands, Kure Atoll, and Johnston Atoll in central Pacific	Eschmeyer & Randall (1975); Matsunuma *et al*. (2017)
D. bellus	Endemic to East Asian continental shelf: South China Sea northward to central Japan, excluding The Philippines & Borneo	Matsunuma *et al*. (2017); Matsunuma *et al*. (2018)
D. biocellatus	Western Indian Ocean from Madagascar, Comoro Islands & Mauritius, eastward through central Indian Ocean to Melanesia, Micronesia & French Polynesia, southward to Australia, northward through southeast Asia to Taiwan & Japan	Matsunuma *et al*. (2017)
D. brachypterus	Eastern Indian Ocean from Maldives, southern India & Sri Lanka, eastward through Andaman Sea, Malaysia, Indonesia, Micronesia & Melanesia to Tonga, southward to Australia & New Zealand, northward through The Philippines & southeast Asia to central coast of Japan	Matsunuma *et al*. (2017)
D. hemprichi	Western Indian Ocean: East coast of South Africa, Madagascar & Seychelle Islands, northward to Somalia, Yemen & Red Sea	Matsunuma *et al*. (2017)
D. koyo	Off Chichi-jima & Ogasawara Islands, Japan	Matsunuma & Motomura (2019)
D. tuamotuensis	Endemic to Tuamotu Archipelago of French Polynesia, central South Pacific Ocean	Matsunuma & Motomura (2013a)
D. zebra	East central Indian Ocean from Seychelles, Réunion & Mauritius, eastward through Thailand, Malaysia, Indonesia & Micronesia to Samoa, southward to Australia, northward to Japan	Matsunuma *et al*. (2017); Matsunuma & Motomura (2019)
Ebosia		
E. bleekeri	Australia northward through Indonesia, The Philippines & Taiwan to central Japan	Eschmeyer & Rama-Rao (1978); Matsunuma & Motomura (2015a)
E. falcata	Indian Ocean: Somalia, Pakistan, east coast of India & Gulf of Mannar, eastward to Andaman Sea	Eschmeyer & Rama-Rao (1978); Matsunuma & Motomura (2015a)

.....Continued on the next page

TABLE 1. (Continued)

Taxon	Distribution	References
E. saya	Possibly endemic to Saya de Malha Bank, western central Indian Ocean	Matsunuma & Motomura (2015a)
E. vespertina	Southwest Indian Ocean: East coast of South Africa to Mozambique & Madagascar	Matsunuma & Motomura (2016b)
Parapterois		
P. heterura	Eastern Indian and western Pacific Oceans: Andaman Sea south to Indonesia & Western Australia, north through The Philippines, Malaysia, Gulf of Thailand, Vietnam, Taiwan & Japan	Matsunuma & Motomura (2022)
P. macrura	Indian Ocean: Arabian & Laccadive Seas (Somalia, Oman, Pakistan & India)	Matsunuma & Motomura (2022)
P. nigripinnis	Southwestern Indian Ocean: East coasts of Mozambique & South Africa	Matsunuma & Motomura (2022)
Pterois		
P. andover	Indonesia & Papua New Guinea	Allen & Erdmann (2008)
P. antennata	East coast of South Africa, Madagascar & Mascarenes, eastward to French Polynesia & Pitcairn Island Group, southward to Australia & Kermadec Islands, northward to Japan	Matsunuma & Motomura (2011); Matsunuma & Motomura (2018)
P. brevipectoralis	Western Indian Ocean: Mascarenes & Saya de Malha Bank east of Madagascar	Mandrytsa (2002); Matsunuma & Motomura (2013b)
P. cincta	Endemic to Red Sea area: Yemen, Saudi Arabia, Egypt, Sudan, Eritrea	Matsunuma & Motomura (2015b); Matsunuma & Motomura (2016a); Matsunuma *et al*. (2016)
P. miles	Indian Ocean: East coast of South Africa, Madagascar & Mascarenes, northward through Red Sea & Persian Gulf, eastward to Malaysia; invasive in Mediterranean Sea & Western Atlantic	Schultz (1986)
P. mombasae [1]	Endemic to Indian Ocean: East coast of South Africa through Indian Ocean to Andaman Sea	Matsunuma & Motomura (2015b)
P. paucispinula [1]	Japan southward through Indonesia to northern Australia, eastward to French Polynesia	Matsunuma & Motomura (2015b); Matsunuma & Motomura (2018)
P. radiata	East coast of South Africa through Micronesia to Tonga, southward to Australia, northward to southern Japan	Matsunuma & Motomura (2015b); Matsunuma & Motomura (2016a)
P. russelii [2]	East coast of South Africa, Madagascar & Mauritius northward to Red Sea & Persian Gulf, eastward through Australia to New Caledonia, northward to Taiwan	Matsunuma *et al*. (2016)
P. sphex	Endemic to Hawai'ian Islands	Eschmeyer & Randall (1975); Matsunuma & Motomura (2015b)
P. volitans [3]	West coast of Australia northward through The Philippines & Indonesia to southern Japan, eastward through Micronesia & Melanesia to Pitcairn Island group; invasive in Western Atlantic	Schultz (1986)

[1] *Pterois mombasae* in Matsunuma & Motomura (2011) is *P. paucispinula* per Matsunuma & Motomura (2015b)
[2] *Pterois lunulata* Temminck & Schlegel, 1843 synonymized as *P. russelii* Bennett, 1831 per Wilcox *et al.* (2018)
[3] Possible hybrid of *P. miles* and *P. russelii*, or recent species resulting from hybridization thereof per Wilcox *et al.* (2018)

Two lionfishes, *Pterois volitans* (Linnaeus, 1758) and *P. miles* (Bennett, 1828), are now invasive in the Western North Atlantic (WNA) with populations of *P. volitans* abundant and widespread (Hunter *et al*. 2021), and those of *P. miles* rare and apparently limited to Atlantic Ocean waters off North Carolina (Hamner *et al*. 2007). We retain existing nomenclature for lionfish populations in the WNA considered to be *P. volitans* because only 1.8% of lionfish tested from the WNA with a suite of molecular markers showed evidence of hybridization between *P. volitans* and *P. miles* (Whitaker & Janosik 2020), and all mtDNA sequences compiled from studies throughout the region correspond to *P. volitans* (Hunter *et al*. 2021).

Most marine invasions result from human-mediated transfers and may go unnoticed until ecosystem impacts occur (Crooks 2005; Evangelista *et al.* 2016). Introduction of invasive species like the predatory lionfishes, however, can adversely impact fishery and aquaculture production, tourism, human health, and the economics of coastal communities (Resiere *et al.* 2016; Papacostas *et al.* 2017). Since first introduced into the WNA, *P. volitans* has reduced the density and biomass of ecologically important reef-associated herbivores, facultative cleaners, marine species that serve as prey for federally managed snapper and grouper stocks, and stocks of other commercially and recreationally important marine fishes (Albins 2015; Dahl *et al.* 2017). Invasion of the Mediterranean Sea by *P. miles* has also adversely impacted that region (Kletou *et al.* 2016; Bariche *et al.* 2017), which heightens concerns that other globally traded species of lionfish pose similar risks if accidently or intentionally introduced into non-native marine ecosystems.

Marine hobbyists can purchase lionfishes sold under at least 10 different "species" names from U.S. vendors or wholesalers, and have them shipped live overnight (Williams *et al.* 2015). Due to high phenotypic plasticity, vendors often use common rather than scientific names to categorize imports, which makes reliable species identification difficult (Cohen *et al.* 2013). Since risks of establishment increase where dispersive mechanisms provide repeated opportunities for introduction, easy access to live ornamentals heightens the possibility of accidental or intentional release of aggressive, predatory species like the lionfishes that may consume tank-mates or outgrow home aquaria (Weigle *et al.* 2005; Johnston & Purkis 2014). Ballast water exchange at high-volume U.S. destination ports further increases risks associated with the potential spread of lionfishes via dispersal of their early life stages (ELS; Kaluza *et al.* 2010).

The lionfishes exhibit a suite of flexible life history traits that enhance survival and dispersal of their ELS (Gunselman & Spruell 2019). In the WNA, *P. volitans* spawn about every 2–3 days year-round, grow rapidly, and mature early (Jud *et al.* 2015; Fogg *et al.* 2017). *Pterois volitans* also displays broad thermohaline tolerances, high trophic plasticity, aggressive feeding behaviors, and an ability to occupy diverse habitats (Byron *et al.* 2014; Grieve *et al.* 2016). After sunset, females release a pair of buoyant, tube-like, gelatinous egg sacs (Mito & Uchida 1958; Matsunuma & Motomura 2016a), which are repulsive to egg predators (Moyer & Zaiser 1981; Koya & Muñoz 2007). Each tube-like sac encapsulates one to two layers of eggs around a hollow core and remains afloat below the surface (Fishelson 1975; Koya & Muñoz 2007). The egg sacs disintegrate within 12–24 hours post-spawning (Fishelson 1975; Moyer & Zaiser 1981) and release the eggs into the water column where larvae hatch within hours to days depending on ambient water temperatures (Mito & Uchida 1958; Smith-Vaniz & Collette 2013). Larvae grow at rates comparable to some high-seas pelagic fishes (Mostowy *et al.* 2020) and remain planktonic for an average of 26–30 days (range: 21–39 days; Ahrenholz & Morris 2010; Lazarre 2016) while wind-driven ocean currents distribute the ELS (Johnston & Purkis 2011).

Despite the threat that lionfishes pose to non-native marine ecosystems worldwide (Sutherland *et al.* 2010), inadequate descriptions of most stages and poorly defined taxonomic characters make their ELS difficult to distinguish from non-pteroine scorpaenids and other morphologically similar taxa. Currently, recognition of ELS of members of *Pterois* relies on a partial description of larvae <2.5 mm notochord length (NL) of *P. lunulata* Temminck & Schlegel, 1843 in Mito & Uchida (1958), now considered to be a synonym of *P. russelii* Bennett, 1831 per Wilcox *et al.* (2018); five larvae described as *P. volitans* from the eastern Indian Ocean (Imamura & Yabe 1996); and four larvae from the Gulf of Mexico and Yucatan Channel molecularly verified as *P. volitans* (Vásquez-Yeomans *et al.* 2011; Kitchens *et al.* 2017). Recognition of larvae of members of *Dendrochirus* relies on eggs and early larvae (1.1–1.9 mm NL) from the Red Sea described as *D. brachypterus* (Cuvier in Cuvier & Valenciennes, 1829) by Fishelson (1975), and an image of a transforming larva (approximately 10.0 mm standard length [SL]; C. Baldwin, pers. comm.) collected in the western Indian Ocean off South Africa labeled *D. brachypterus* in Baldwin (2013: 540, fig. 40E). Recently, however, Matsunuma *et al.* (2017) described populations of *D. brachypterus* from the western Indian Ocean and Red Sea as *D. hemprichi* Matsunuma, Motomura & Bogorodsky, 2017. Kojima

(2014) described a 9.5 mm SL larva of *D. bellus* (Jordan & Hubbs, 1925), an identification Matsunuma *et al.* (2017) considered uncertain because distributions and meristics overlap those of *D. brachypterus* in waters off Japan (Table 1), and diagnostic characters to distinguish their larvae are unknown. Pending description of molecularly verified larvae of *D. brachypterus* and *D. bellus*, or further evidence to corroborate the identity of Kojima's (2014) larva, we hereafter refer to the 9.5 mm SL larva as *D.* "*bellus*." Shadrin & Emel'yanova (2019) provided a partial description of embryonic and early preflexion larvae of *D. zebra* (Cuvier in Cuvier & Valenciennes, 1829), and Kojima (2014) described a 11.5 mm SL larva, and Matsunuma & Motomura (2019) a 14.0 mm SL juvenile *D. zebra*. Larvae of *D. barberi* (Steindachner, 1900) have not been described.

Identification of characteristics to recognize and distinguish pteroine ELS from those of non-pteroine scorpaenids may reveal species and life-stage specific differences in ecological requirements, dispersal pathways, and habitat-use patterns that enable development of alternate management strategies to reduce the socioeconomic impacts of lionfishes on human health and coastal communities (Côté *et al.* 2013). Proactive biomonitoring of WNA waters for introduction of other invasive members of *Pterois* and *Dendrochirus*, however, will require the ability to recognize and distinguish their ELS from those of other pteroine and non-pteroine scorpaenids. Our goals were to: comparatively describe larvae of *P. volitans* and *D. barberi*, and two transforming larvae and an early juvenile of *D. hemprichi*; review information on the early development of *D. zebra* and a larva described as *D.* "*bellus*"; and identify characteristics to distinguish *P. volitans* from the four members of *Dendrochirus*. We also provide new information for small juveniles of two poorly known non-pteroine scorpaenids from the WNA, and discuss characteristics that distinguish the five pteroines from non-pteroine scorpaenid genera and morphologically similar taxa. We restrict comparisons to scorpaenids found in subtropical and temperate waters of the WNA, but include information on other non-native pteroine genera in hopes of stimulating further interest and research on the ELS of the lionfishes.

Material and methods

We examined *P. volitans* larvae collected during multiple fisheries surveys of Gulf of Mexico and Western Caribbean waters, and during Deepwater Horizon (DWH) oil spill monitoring of the Gulf of Mexico conducted by the National Oceanographic and Atmospheric Association (NOAA). In general, the aforementioned zooplankton collections employed 60 cm bongo nets fitted with 0.333 mm or 0.505 mm mesh nets towed obliquely from 200 m to the sea surface. Samples collected during DWH oil spill monitoring included discrete depth tows taken with either a 1 m^2 Multiple Opening and Closing Net Environmental Sensing System (MOCNESS) sampler fitted with 0.505 mm mesh, or a 10 m^2 MOCNESS fitted with 3 mm mesh. Tows were taken whenever the ship occupied a given station regardless of time of day. Samples were fixed initially in formalin or placed directly into 95% ethanol at sea, returned to the laboratory for sorting, and preserved in 85–95% ethanol for long-term storage.

Of the nine *P. volitans* larvae from which we obtained morphometric, meristic, and other developmental information, only the 3.9 mm SL larva mentioned in Kitchens *et al.* (2017) and included here was molecularly verified. Supplemental material examined included digitized images of *P. volitans* collected during multiple ichthyoplankton surveys of the Western Caribbean archived in the Zooplankton Museum at El Colegio de la Frontera Sur (ECOSUR), Unidad Chetumal, Mexico. Illustrations of *P. volitans* larvae were modified from Levine (2015: fig. 1) to depict cranial and opercular spination patterns more accurately during early development. Although larvae were catalogued, sequences were not archived in BOLD or GenBank.

Larvae of *D. barberi* were originally collected by Clarke (1991) during 1978 and 1979 off O'ahu, Hawai'i, and obtained from the Los Angeles County Museum of Natural History (LACM) (Appendix Table 1). The LACM collections also contained a 21.0 mm SL juvenile captured during 1970 off South Sail Rock Channel, Kenya, and catalogued as *Dendrochirus* sp., which we identified as *D. hemprichi*, which we identified as *D. hemprichi* based on characters described in Matsunuma *et al.* (2017). We also examined images of two transforming larvae of *Dendrochirus* sp., which we identified as *D. hemprichi* (estimated SL: 10.0 & 11.0 mm) based on morphology, collection location, and species distribution information in Matsunuma *et al.* (2017). Pigmentation patterns and other characteristics observed in those images provide the basis for our description of transforming *D. hemprichi*. The 10.0 mm SL larva collected off Kenya was labeled *D. brachypterus* in Baldwin (2013), whereas the 11.0 mm SL larva was collected in the Red Sea. For comparison purposes, Kojima's (2014) descriptions of a 9.5 mm SL *D.*

"*bellus*" and 11.0 mm SL *D. zebra* were translated from Japanese to English, and are summarized here. Kojima (pers. comm.) also kindly provided an image of the head of a cleared and stained *D.* "*bellus*" larva from which we were able to verify additional details not depicted in his illustration.

Counts and body measurements were taken on the left side of the body where possible. We considered NL in preflexion larvae synonymous with SL, and recorded all lengths as mm SL, unless noted otherwise. Morphometrics were recorded to the nearest 0.1 mm from images of *P. volitans* and *D. barberi* captured with a Nikon AZ100M microscope and camera package with Nikon Imaging Software-Elements, Basic Research (NIS Elements BR) measurement software, or a stereo-zoom microscope equipped with calibrated ocular micrometer. We made most measurements parallel or perpendicular to the longitudinal axis of the body, except maxilla depth, which we measured across the deepest part of the maxilla near its terminal margin, regardless of orientation. We measured maxilla length horizontally from the snout tip to a vertical line through the terminal margin of the maxilla, and measured pectoral-fin base depth from the uppermost to lowermost pterygiophore. "Soft" dorsal and anal fins refer to the rayed portions only. We present relative changes in body shape as ratios [% SL, head length (% HL), orbit diameter (% OD), and body depth at cleithrum (% BDc)] because species descriptions often use ratios as the primary means to distinguish cryptic and closely related taxa when other qualitative characters are ill-defined (Baur & Leuenberger 2011).

We followed the widely accepted and commonly used terminology of Ahlstrom *et al*. (1976) to categorize "stages" of development based on orientation of the notochord tip (e.g., preflexion, flexion, postflexion). "Preflexion" stage is self-explanatory. "Flexion" stage begins when the notochord turns upward, and coincides or nearly so with initial development of the hypural bones and primary rays of the caudal fin. Alignment of the medial caudal rays with the longitudinal axis of the body and attainment of a full complement of primary rays initiate the "postflexion" stage, which includes a transitional or transformational period of changes in morphology and pigmentation leading to the juvenile life phase. We refer to larvae undergoing this transition as "transformers." As defined here, transformation is the dynamic process during which larvae undergo a period of irreversible physiological change that includes endocrine mediators, remodeling of the overall phenotype, and involves multiple traits (e.g., alimentary and sensory systems, pigmentation patterns, allometric changes in head and body shape). The transformation process also typically includes resorption or loss of species-specific, specialized larval characters, and development of new traits that permit exploitation of a different ecological habitat or niche (McMenamin & Parichy 2013). Settlement to the adult habitat generally coincides with initiation of the juvenile phase for most benthic fishes (Leis & Carson-Ewart 2000).

Branchiostegal-ray (BR) and fin-element counts, and observations of cranial and opercular spination patterns often required the addition of cyanine blue stain to enhance details. Terminology for cranial and opercular spination (Fig. 1) is modified from Moser (1996). We counted pterygiophores in early larvae because developing spines and rays are fragile and easily damaged during sample collection and specimen handling. Bases of soft-rayed pterygiophores are typically rounded or columnar, contiguous or nearly so, and larger than those of spines, which appear triangular, non-contiguous, and smaller (Leis & Carson-Ewart 2000). The element associated with the third pterygiophore of the anal fin forms first as a ray and was counted as such until transformed into a hardened structure (i.e., third anal spine); consequently, we used the pterygiophore of the fourth element (i.e., first "true" ray) to evaluate the relative position of the anteriormost soft ray of the anal fin. Pectoral-fin rays were numbered from uppermost to lowermost, and pelvic-fin rays from innermost to outermost to determine placement of pigment.

Designations of spine length along the posterior shelf of the preopercle (PPO) are based on those considered "typical" or "representative" of the genus, although some variability should be expected for species-rich taxa. We define PPO spine length as follows: "short" (equal to or less than pupil diameter); "moderate" (length greater than pupil diameter to not more than tip slightly beyond the outer margin of the operculum); and "elongate" (about two or more times longer than the next longest spine, or extending well beyond the posterior margin of the operculum or ventral margin of the body, depending on orientation). "Robust" spines refer to "elongate" spines, as defined above, that are also structurally stout and broad-based, whereas spines of short to moderate length are typically "slender," with a relatively narrow base. "Elongate" fins are those whose rays extend to and typically well beyond the terminal margin of the anal-fin base as compared to "short" fins that may extend to, but seldom beyond, the origin of the anal-fin base. Institutional abbreviations follow Sabaj (2020). Although some authors elevate subfamilies within Scorpaenidae to family level (e.g., Sebastidae, Setarchidae), we retain the subfamily nomenclature of van der Laan *et al*. (2023) pending consensus acceptance of a revised classification.

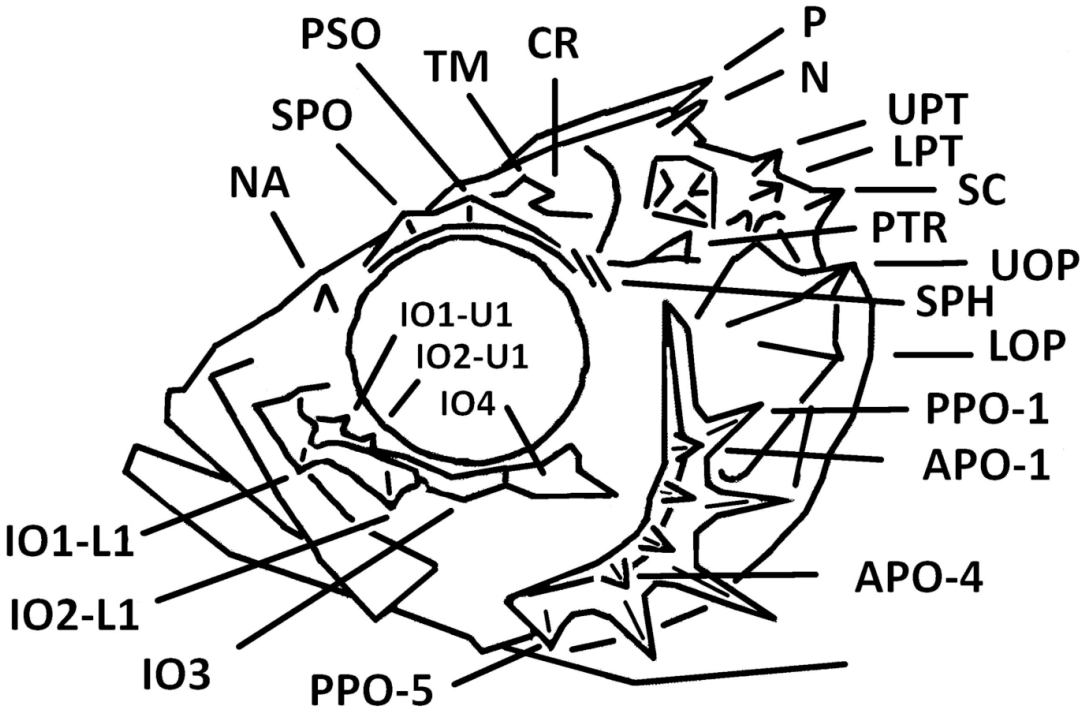

FIGURE 1. Typical scorpaenid cranial and opercular spination modified from Moser (1996). Abbreviations: spines 1–4 along anterior shelf of preopercle (APO); spines 1–5 along posterior shelf of preopercle (PPO); APO and PPO spines numbered from uppermost to lowermost; nuchal (N); parietal (P); coronal (CR); tympanic (TM); postocular (PSO); supraocular (SPO); nasal (NA); lower spine on opercle (LOP); upper spine on opercle (UOP); sphenotic ridges (SPH); pterotic ridge/spine (PTR); supracleithral ridge/spine (SC); posttemporal ridges and spines on upper (UPT) and lower (LPT) margins; infraorbital ridge (IO) comprised of bones 1 through 4, and associated spine on lower (L) or upper (U) margin.

The terms melanophore(s) and pigment(s) are used interchangeably throughout the text because the chemicals used to prepare specimens bleach the chromatophores during the fixation and preservation process, and only the brown or black pigments or melanin remain (Leis & Carson-Ewart 2000). We define the "types" of pigmentation as follows:

Bar or band: a relatively broad, progressively elongate vertical or diagonal pattern of darker pigment separated by an area of lighter pigment;

Blotch: an enlarged, often circular melanophore, or aggregation of "close-set" melanophores arranged in a roughly circular pattern that differs in shape or intensity from surrounding pigment;

Mottled: a combination of tens to hundreds of individual melanophores of different intensities that produce a pattern of irregular size or shape;

Saddle: a pattern that wraps around the dorsal or ventral margin(s) of the body;

Shield: the extent of pigmentation over the dorsolateral surface of the visceral mass in early larvae of some scorpaenids, which in larger larvae may be reduced in size and intensity, or augmented with scattered blotches of pigment;

Stripe: a "line" of pigment along the longitudinal axis of the body or perpendicular to the dorsal surface of the head that maintains a nearly consistent width along its length and differs in intensity from surrounding pigment;

Swath or Streak: a concentration of "close-set" melanophores of relatively uniform intensity that forms an area of pigment elongate in shape.

Results

Pterois volitans: general morphology

We measured nine *P. volitans* larvae from 2.5–12.9 mm (Fig. 2a–g) and examined others as supplemental material. Smallest preflexion larva characterized by precocious pectoral fins, deep base, elongate rays. Gut with single loop or "twist" (Fig. 2a), and terminates slightly beyond mid-body; hindgut becomes rugose in early postflexion larvae. Flexion larvae with tips of longest developing pectoral rays to or beyond posterior margin of dorsal-fin base; by early postflexion, these rays extend to about terminal margin of caudal peduncle (CP) or beyond, if unbroken. Flexion larvae with pronounced "hump" in snout dorsal profile created by elevation of rostral cartilage (i.e., ascending process of premaxilla). Head deep, angle of lower jaw pronounced; snout typically 10–15% shorter than OD; CP shortens, deepens as notochord flexes. Upper jaw terminates near mid-orbit; maxilla deepens near terminal margin, its maximum depth >55% OD. CP depth nearly equal to its length in postflexion and transforming larvae (Table 2). Seven BR.

Pigmentation

Pigmentation sparse in all larvae examined (Fig. 2a–e). Internally, head with melanophore between lobes of midbrain in smallest larva, and on dorsoposterior surface of hindbrain and brainstem by 3.0 mm. Flexion larvae add pigment to ventrolateral surface of each lobe of hindbrain (otic region), which together with midbrain pigment forms "triangular" pattern when viewed downward from top of head (Kitchens *et al.* 2017: fig. 3). Early postflexion larvae (~5.0 mm) with series of subsurface melanophores across dorsoposterior margin of midbrain, and dorsal and lateral surfaces of hindbrain and brainstem; this pigment gradually obscured by cranial ossification and thickening musculature in early transformers (~10.0 mm). Behind head, pigment on dorsoposterior margin of hindgut near anus in smallest larva (Fig. 2a) becomes more conspicuous in flexion larvae. Dorsal surface of visceral mass along body wall lightly pigmented at all sizes; dorsal surface of gas bladder unpigmented until early postflexion. All internal pigment gradually obscured by thickening abdominal musculature in early transformers.

Externally, pigment concentrated along body midlines. Pigmentation in preflexion larvae varies from opposing dorsal and ventral blotches to narrow longitudinal swath located along posterior third of body margins; lateral midline with one to three "dash-like" melanophores (Fig. 2a). Flexion larvae with pigment typically restricted to narrow longitudinal swath about 4–5 epimeres wide near posterior margin of developing dorsal-fin base; another swath about 2–3 hypomeres wide near posterior margin of developing anal-fin base; and mid-lateral series of 3–5 "dash-like" pigments along CP. One of two flexion larvae with small pair of melanophores embedded in ventral midline of CP anterior to developing hypural elements; a single melanophore embedded between upper and lower hypural plates, and pigment scattered over lower plate (Kitchens *et al.* 2017: fig. 3); pigment lacking at these locations in postflexion larvae. Swath of pigment along body margin and posterior half of soft dorsal-fin base, and above posterior third of anal-fin base, extends onto adjacent 1–2 myomeres of CP in postflexion larvae. By 6.0 mm, series of 3–4 melanophores added near mid-base of developing spinous dorsal fin, these pigments on pterygiophores 9 through 11 in 8.5 mm larva (Fig. 2c). Pigmentation unchanged to slightly reduced along dorsal, lateral, and ventral body thereafter until early transformation. During that period, pigment typically restricted to narrow "dash-like" series of melanophores below soft dorsal-fin base and along margin of adjacent epimeres, 0–3 melanophores along lateral midline of CP, and along last 3–4 pterygiophores of anal-fin base. Early transformers add pair of enlarged melanophores to dorsal surface of head between parietal spines (Fig. 2f); single melanophore to small cluster along dorsal rim of premaxilla; and single to short series of melanophores along dorsal midline near mid-CP. Pigment along anal-fin base typically reduced to one or two melanophores, often large, on lateral surface of penultimate and antepenultimate pterygiophores. Largest transformer (12.9 mm) adds enlarged melanophore or blotch to surface of head (midbrain region), and small cluster to snout between anteroventral margin of orbit and upper lip.

TABLE 2. *Pterois volitans*, *Dendrochirus barberi*, and *D. hemprichi* morphometrics by life stage. Mean (range). Abbreviations: standard length (SL); head length (HL); orbit diameter (OD); body depth at cleithrum (BDc); caudal-peduncle depth at terminal margin of dorsal-fin base (CPD); caudal-peduncle length (CPL); posterior shelf of preopercle (PPO); character not developed (ND). Asterisk indicates morphometric not available due to specimen damage. Dorsal-fin base length to SL ratio excluded for the aberrant 12.9 mm *P. volitans* larva lacking first three dorsal spines and associated structures.

Character (expressed as designated ratio)	***Pterois volitans***			***Dendrochirus barberi***	***Dendrochirus hemprichi***
	Preflexion	**Flexion**	**Postflexion/ Transformers**	**Postflexion/ Transformers**	**Juvenile**
Number of specimens	1	2	6	12	1
Standard length (mm)	2.5	3.6–3.9	5.9–12.9	8.6–14.0	21.0
Head length (% SL)	36%	38–43%	32 (31–33%)	32 (29–35%)	38%
Orbit diameter (% HL)	32%	31–33%	34 (30–36%)	37 (33–40%)	40%
Snout length (% OD)	90%	85–92%	91 (82–100%)	70 (63–77%)	63%
Longest preopercular spine (% OD)	ND	48–51%	49 (40–65%)	29 (20–36%) [1]	25% [2]
Upper-jaw length (% HL)	46%	49–52%	47 (43–54%)	49 (45–53%)	54%
Maximum depth of maxilla (% OD)	*	56–57%	62 (58–67%)	49 (45–55%)	44%
Preanal length (% SL)	56%	59–61%	60 (59–62%)	62 (58–65%)	67%
Body depth at cleithrum (% SL)	20%	32–34%	29 (27–32%)	34 (30–37%)	43%
Maximum depth of pectoral-fin base (% BDc)	*	55–56%	54 (52–58%)	49 (44–54%)	39%
CPD at dorsal-fin base termination (% SL)	ND	12–13%	14 (13–15%)	17 (16–19%)	14%
Caudal-peduncle length (% SL)	ND	17–20%	15 (12–16%)	15 (13–16%)	11%
CPL/CPD ratio	ND	61–71%	93 (89–100%)	84 (75–90%)	75%
CPD/BDc ratio	ND	36–38%	50 (48–52%)	51 (49–53%)	36%
Snout tip to pelvic-fin base (% SL)	ND	36%	32 (29–34%)	35 (33–38%)	34%
Dorsal-fin base length (% SL)	ND	18–21%	56 (50–61%)	55 (52–59%)	60%
Ratio of 1st/2nd dorsal spine length	ND	ND	49% [3]	100% / 76% [4]	75%
Ratio of 1st/2nd anal spine length	ND	ND	61–64% [5]	55 (46–67%)	50%
Anal-fin base length (% SL)	ND	13–15%	22 (20–24%)	20 (17–21%)	18%
Snout tip to 1st dorsal pterygiophore (% SL)	ND	ND	32 (29–35%)	29 (25–32%)	26%
Snout tip to last anal pterygiophore (% SL)	ND	72–81%	83 (80–85%)	82 (78–84%)	87%
Pelvic-fin origin to 1st anal pterygiophore (% SL)	ND	22–28%	28 (26–31%)	27 (25–32%)	32%

[1] Upper four spines along preopercle subequal
[2] Longest PPO spine is uppermost (PPO-1)
[3] Only one larva with first & second dorsal spines developed & intact
[4] Only one postflexion & one transforming larva with both dorsal spines intact
[5] Only two larvae with first & second anal spines developed & intact

Fin development and pigmentation

Pectoral fins precocious, base deep, typically 53–56% BDc (Table 2); all rays present in early postflexion larvae (Table 3). Pigment lightly scattered over mid- to outer-margin of blade and developing rays in flexion larvae, and beginning to consolidate into irregularly shaped patches in postflexion larvae. By 7.0–8.0 mm, scattered pigment at several locations along inner third to mid-shaft of fins, on webbing between rays, on inner third of shaft only of rays 4–6, and near mid-shaft of rays 13–14; early transformers add pigment along outer third of shaft of most rays. Tips of longest unbroken rays extend to or slightly beyond terminal margin of CP through late postflexion; pectoral fins become relatively shorter during transformation.

Early postflexion larvae with three to four rays in pelvic fin, and all elements by 7.0 mm (Table 3). By 8.5 mm, pigment on outer third of webbing between pelvic spine and outermost ray (Fig. 2d); tips of middle three rays extend to or slightly beyond first pterygiophore of anal-fin base. By 11.0 mm, longest pelvic rays extend to or beyond mid-anal-fin base, with part of innermost ray attached by short membrane to abdominal wall; tip of pelvic spine when pressed against body extends to or slightly beyond first pterygiophore of anal-fin base.

Bases of soft dorsal and anal fins thickening outward from mid-base in flexion larvae. Early postflexion larvae with all dorsal- and anal-fin pterygiophores, and most elements developing; full complement of elements present by 8.0 mm (Table 3). First and second spines of anal fin formed by 7.0 mm; tips of last 3–4 soft dorsal rays, last two rays of anal fin now extend to or slightly beyond terminal margin of hypural plate. Gap between first and second dorsal spines narrower than between subsequent spines, length of first spine about one-half that of second spine; length of first anal spine <65% that of second (Table 2). Pterygiophore of first dorsal spine typically inserted over operculum. If 13 dorsal spines, first anal spine inserted below 12th to 13th spine; if 12 spines, first anal spine inserted below 12th spine to first ray of soft dorsal fin. First "true" ray of anal fin (fourth element) inserted below first to second ray of soft dorsal fin; terminal pterygiophore of anal fin inserted below penultimate to antepenultimate pterygiophore of soft dorsal fin. Caudal fin with 7+7 primary rays by 8.0 mm; early transformers with 22 total caudal-fin elements (Table 3).

TABLE 3. *Pterois volitans*, *Dendrochirus barberi*, and *D. hemprichi* meristics by life stage. Counts represent the number of pterygiophores or developing elements along the respective fin base. Numbers in parentheses denote rare counts. ND: character not developed. Third element of anal fin does not transform into third anal spine until after settlement.

Metric	*Pterois volitans*				*Dendrochirus barberi*		*D. hemprichi*
	Preflexion	**Flexion**	**Postflexion**	**Transformers**	**Postflexion**	**Transformers**	**Juvenile**
Number of specimens	1	2	5	1	4	6	1
Standard length (mm)	2.5	3.6–3.9	5.9–10.2	12.9	8.6–9.2	10.6–14.5	21.0
Dorsal-fin elements (spines, rays)	ND	0, 10	(XII) XIII, 11 (12)	IX, 12 [1]	XII, 10	XIII, 9	XIII, 9
Anal-fin elements (spines, rays)	ND	0, 0–8	II, 8	II, 8	II, 6	II, 6	III, 5
Pectoral-fin elements (left, right side)	ND	Anlage	14, 14	14, 14	17 right	17 right	17 right
Pelvic-fin elements	ND	Buds	3 rays to I, 5	I, 5	I, 5	I, 5	I, 5
Primary caudal-fin elements	ND	Anlage	7 + 7	7 + 7	7 + 7	7 + 7	7 + 7
Secondary caudal-fin elements	ND	ND	0–1 + 0–1	3 + 3	0–1 + 0–1	2–3 + 2–3	3 + 3

[1] Aberrant larva lacking anterior three dorsal spines & associated structures

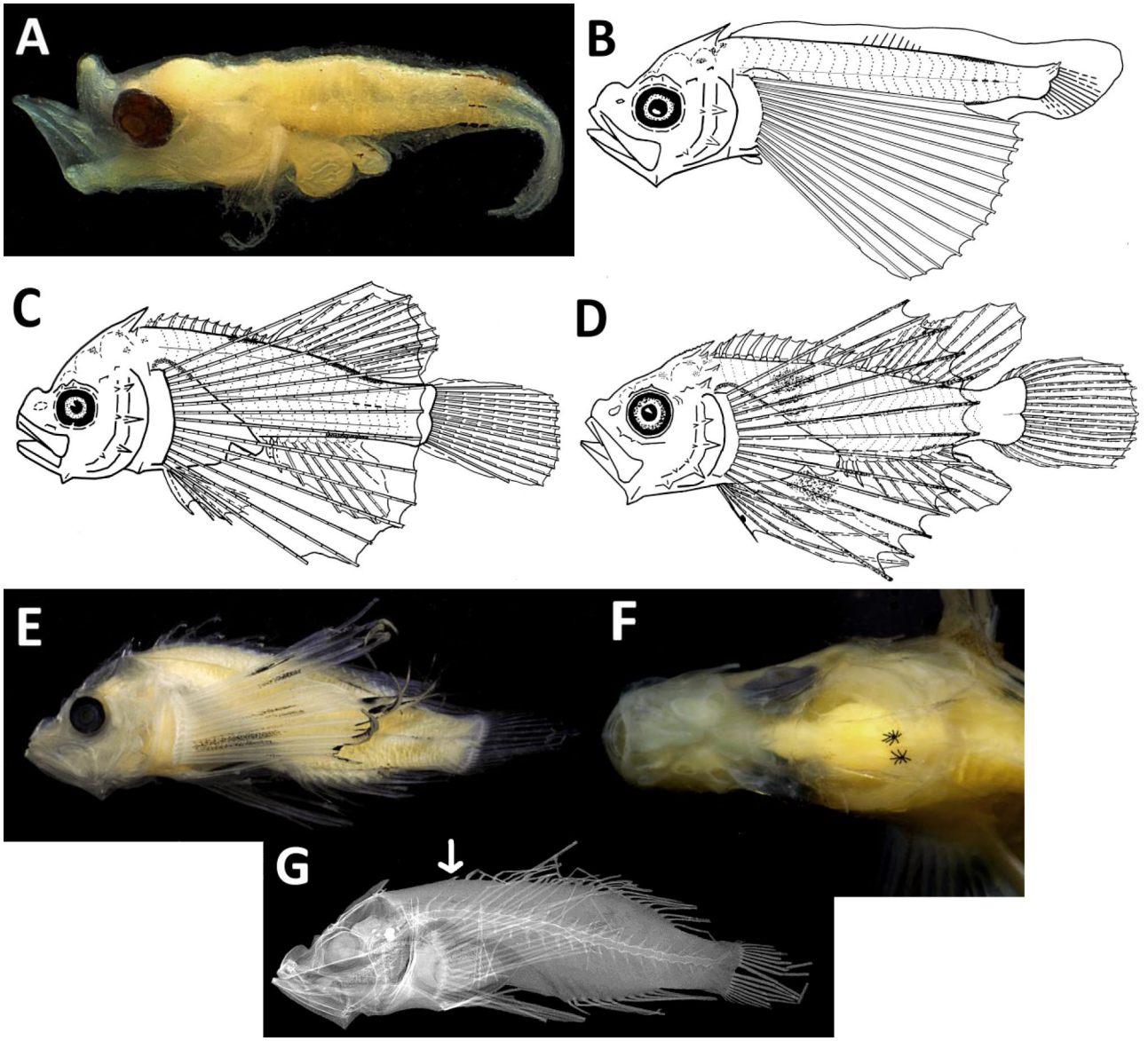

FIGURE 2. *Pterois volitans* larvae. A. 2.5 mm; B. 4.6 mm (pectoral-fin pigment omitted due to broken rays in larva illustrated); C. 6.0 mm; D. 8.5 mm; E. 9.3 mm; F. 9.8 mm; G. radiograph of aberrant 12.9 mm larva lacking first three dorsal spines and associated structures; arrow indicates position of anteriormost pterygiophore and underdeveloped fourth dorsal spine. All lengths in mm standard length (SL) post-preservation. Pigmentation enhanced in some images for illustration and detail purposes.

Largest transformer with aberrant number of dorsal-fin elements (21 total, typical count 23–24; Table 3), lacks first three pterygiophores and associated structures, fourth pterygiophore underdeveloped. Origin of spinous dorsal fin displaced posteriorly, anteriormost pterygiophore (fourth) located over dorsal splay of sixth epimere (Fig. 2g); third element of anal fin untransformed; dorsal, anal, and caudal fins unpigmented in largest transformer.

Cephalic and opercular spination; supraocular and nasal cirri; and sensory pore development

Number, relative length, and orientation of PPO spines change as larvae develop. Smallest larva with small PPO-2 along upper margin, and PPO-3 along lower margin. Flexion larvae add two small spines along anterior shelf of preopercle (APO), APO-2 along upper margin behind lower rim of orbit, and APO-4 along lower margin near angle of lower jaw (Fig. 3a). Early postflexion larvae add small APO-1 and PPO-1 along upper margin, and add APO-3

and PPO-4 along lower margin by 7.0 mm. APO spines 1 through 3 generally overlay their PPO counterparts, with APO-4 inserted between PPO-3 and -4, but closer to PPO-4. PPO-1 directed toward upper margin of opercle, PPO-2 nearly horizontal, PPO-3 directed toward pelvic-fin base, PPO-4 directed ventrally (Fig. 3b). PPO-2 and -3 similar in length, longer than -1 and -4; mean length of PPO-2 and -3 about 50% OD in flexion and early postflexion larvae (Table 2). PPO-4, shortest, length less than one-half that of PPO-2 and -3; all PPO's regress in length relative to OD during transformation. By 8.5 mm, cephalosensory canal along outer margin of PPO with three pores: uppermost near PPO-1, middle pore between -1 and -2, lowermost pore between -2 and -3 (Fig. 3c). By 11.0 mm, sensory canal added along ventral margin of infraorbital ridge with five pores. Largest transformer with lateral margins of PPO-1 through -3 weakly serrate; opercle, interopercle, and subopercle lack spines at sizes examined.

Most cranial ridges and spines indistinct in preflexion larvae, and weakly developed in flexion and early postflexion larvae. Pair of small dorsoposteriorly directed parietal spines present in late preflexion larvae; flexion larvae with pterotic, lower posttemporal, supraocular, and postocular ridges developing; pterotic ridge with short medial spine. Height of pterotic ridge increases toward posterior margin, short spine on terminal margin in early postflexion larvae; terminal margin of lower posttemporal ridge with short spine by 7.0 mm. Pterotic ridge two times longer, higher than lower posttemporal ridge at 7.0 mm, pterotic ridge nearly three times longer by 8.5 mm. Largest transformer, however, with lower posttemporal ridge longer, and two times higher than pterotic ridge. Transformers also add vertical pair of short, parallel, irregularly sculpted sphenotic ridges behind orbit.

Nuchal spines short, acute, conjoined to outer margin of parietal base in flexion larvae, parietals longer than nuchals, both elevated and directed upward about 30° above longitudinal axis of head. Parietal spines over two times longer than nuchals by 8.0 mm (Fig. 3a-c), about three times longer by 10.0 mm; both spines gradually regress during transformation. By 8.5 mm, larvae with anterior margin of parietal spines weakly dentate; posterior margin of parietals, and anterior and posterior margins of nuchals smooth in all examined.

Supraocular and postocular ridges continuous in early postflexion larvae, supraocular ridge low, postocular ridge rises abruptly along anterior margin to acute peak near mid-orbit, ridge height decreases thereafter along dorsoposterior margin of orbit. Supraocular and postocular ridges project outward above orbits like "blinders," postocular more so than supraocular ridge. By 8.5 mm, supraocular ridge broadly rounded, small spine near terminal margin, ridge height about one-half that of postocular. Early transformers with anterior margin of postocular ridge weakly dentate, spine midway along ridge.

Lateral ridge along first infraorbital (IO1) low, poorly developed; small spine on anterodorsal (upper, U) margin (IO1-U1) by 7.0 mm, and on anteroventral (lower, L) margin (IO1-L1) by 8.0 mm (Fig. 3b–c). Lateral ridge crosses onto second infraorbital (IO2) by 8.5 mm, spine on its posteroventral margin (IO2-L1) by 10.0 mm; lateral ridge crosses third infraorbital (IO3) in early transformers; and terminates on fourth infraorbital (IO4) below posterior margin of orbit, small spine on its terminal margin by 11.0 mm. Transformers add weak outer interorbital and upper posttemporal ridges. Outer interorbital ridge connects to coronal base, bifurcates terminally into low coronal (inner) and tympanic (outer) ridges; both ridges lack spines and serrations in all examined. Transformers also add short, unpigmented supraocular cirrus, and small, unpigmented nasal cirrus along dorsal rim of lower nostril by 11.0 mm. Largest transformer with small, blunt spine on terminal margin of upper posttemporal ridge.

Dendrochirus barberi: general morphology

We measured 12 postflexion and transforming larvae from 8.6–14.0 mm (Fig. 4a–e). Mean HL 32% SL; snout length typically 65–75% OD; mean BDc 34% SL; body depth at CP 51% BDc; CP about 15% deeper than long (Table 2). Rays of pectoral fin elongate, tips of longest extend to or slightly beyond last pterygiophore of dorsal-fin base in smallest larva; mean depth of pectoral-fin base 49% BDc (Table 2). All larvae with pronounced "hump" in dorsal profile of snout due to elevated rostral cartilage; terminal margin of maxilla extends to about mid-orbit. PPO spines about evenly spaced along shelf margin, upper 3–4 subequal, lowermost shortest (Fig. 4a). Smallest larva with oblong loop in fore- and mid-gut; hindgut slender, terminates beyond mid-body; gut with rugose folds in early transformers (~9.0 mm). Gas bladder unpigmented, obscured by abdominal musculature in transformers. Seven BR.

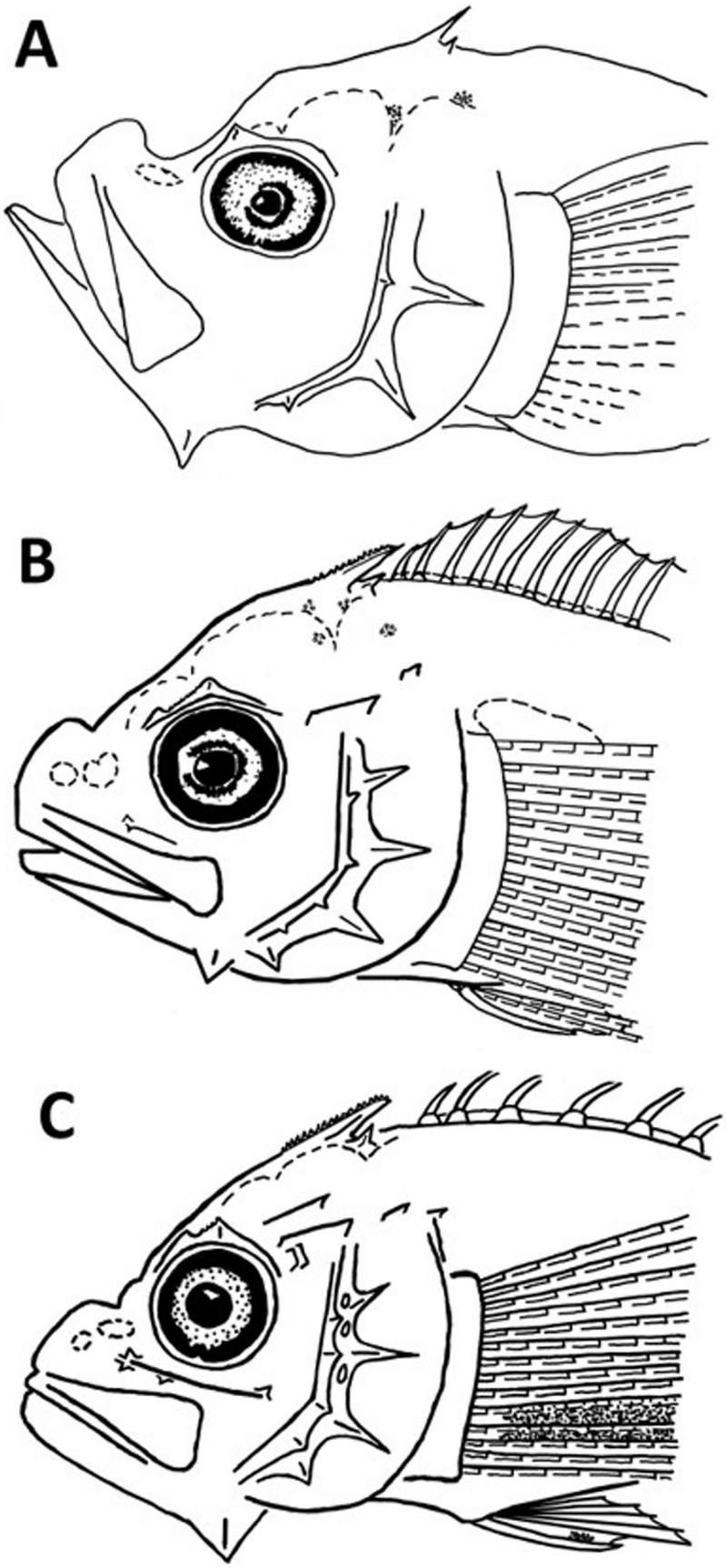

FIGURE 3. Cranial and opercular spination in *Pterois volitans* larvae. A. 3.6 mm; B. 8.0 mm; C. 9.3 mm (pelvic fins not to scale). All lengths in mm standard length (SL) post-preservation.

Pigmentation

Head and visceral mass unpigmented or nearly so, body sparsely pigmented until early transformation (Fig. 4b). Smallest postflexion larva (8.6 mm) with pigment on dorsolateral surface of hindgut, this pigment obscured by thickening abdominal musculature in largest transformer (Fig. 4c-e). Externally, early transformers with small pigment on pterygiophore of 10th dorsal spine, and third and last two pterygiophores of soft dorsal-fin base; expanded melanophore on third, fourth, and last two pterygiophores of anal-fin base; and small ventral blotch near mid-CP (Fig. 4c). Laterally, series of three close-set "dash-like" melanophores along body midline on penultimate and antepenultimate myomeres of CP, which by 11.0 mm, coalesce into narrow, elongate streak. Transformers also add large circular melanophore to dorsal surface of head (midbrain region), small cluster to anterodorsal margin of upper lip, and five partial saddles along dorsal margin of body: anterior saddle near origin of spinous dorsal fin, posterior saddle near terminal margin of soft dorsal-fin base (Fig. 4c-e). By 11.0 mm, CP with dorsal series of three melanophores perpendicular to longitudinal axis of body near mid-peduncle, one medial and one on each side of body midline; another pigment embedded in CP midline near anteriormost developed upper secondary element. By 12.0 mm, two stripes present across head: anterior stripe between orbital margins, posterior stripe between bases of parietal spines. Small dorsal blotch also added near mid-CP, its position about one myomere caudad of opposing blotch on ventral margin. Largest transformer (14.0 mm) adds pigment on snout near upper lip, dorsal margin of lower lip near symphysial knob, angle of lower jaw, near anteroventral and ventral margins of orbit, to cheek near lower margin of APO, and diagonal streak between posterior margin of orbit and APO (Fig. 4e). Ventrolateral margin of lower lip lightly mottled near mid-lip.

Fin development and pigmentation

Smallest larva with full complement of pterygiophores in dorsal- and anal-fins; caudal fin with 5+5 weakly segmented, and 2+2 unsegmented rays (Table 3). Dorsal and anal spines feeble, first two dorsal spines of similar length, last three elements of spinous dorsal fin ray-like. Pterygiophore of first dorsal spine inserted above lower posttemporal ridge; gap between first and second dorsal spine narrower than between subsequent spines. Tips of dorsal- and anal-fin rays from behind about mid-base extend to terminal margin of hypural plate. Transformers with all dorsal spines and first two anal spines well developed, and a full complement of 7+7 primary caudal rays (inner 6+6 segmented), plus 3+3 secondary elements (20 total as in adults). Second dorsal spine about 25% longer than first; second anal spine nearly two times longer than first; third element of anal fin ray-like, untransformed in largest larva. Pterygiophore of first anal spine inserted below 12th to 13th dorsal spine; if 12 spines, inserted below 12th dorsal spine to first ray. Pterygiophore of first "true" ray of anal fin inserted below first to second ray of soft dorsal fin, terminal pterygiophore of anal-fin base inserted below penultimate to antepenultimate pterygiophores of soft dorsal fin. Largest transformer adds pigment along outer third of shaft of first and second dorsal rays, and shaft and on membrane between fourth through sixth rays of anal fin. Last ray of dorsal fin attached by short membrane to body wall, last anal ray free; caudal fin unpigmented in largest transformer.

Smallest larva with all pectoral- and pelvic-fin elements well formed. Although upper four rays of pectoral fin broken off near mid-shaft, diffuse blotch of pigment on inner third of shaft and membrane between rays 5–6, 10–11, and along outer margin of shaft and membrane between rays 7–8. Early transformers with pigment along shaft and membrane of rays 2–3, near outer third of shaft of rays 9–11, and near outer margin of rays 12–15 (Fig. 4c). Largest transformer with pigment consolidating into series of oblong blotches in two uneven rows near mid-fin and outer margin (Fig. 4e); lower four rays of pectoral fin slightly thickened; longest rays extend to or slightly beyond last pterygiophore of dorsal-fin base.

Tips of longest rays of pelvic fin extend to or slightly beyond mid-anal-fin base, innermost ray joined to abdomen by short membrane in smallest larva. Pigment on inner third of membrane that connects innermost ray to abdominal wall, this pigment more pronounced in transformers. By 11.0 mm, pigment present near mid- and outer-margin of shaft of innermost ray, and along outer 25% of shaft and on membrane between rays 3–4; pelvic spine extends <70% of distance to origin of anal-fin base when pressed against body. Late transformers with pigment on webbing between pelvic spine and outermost ray.

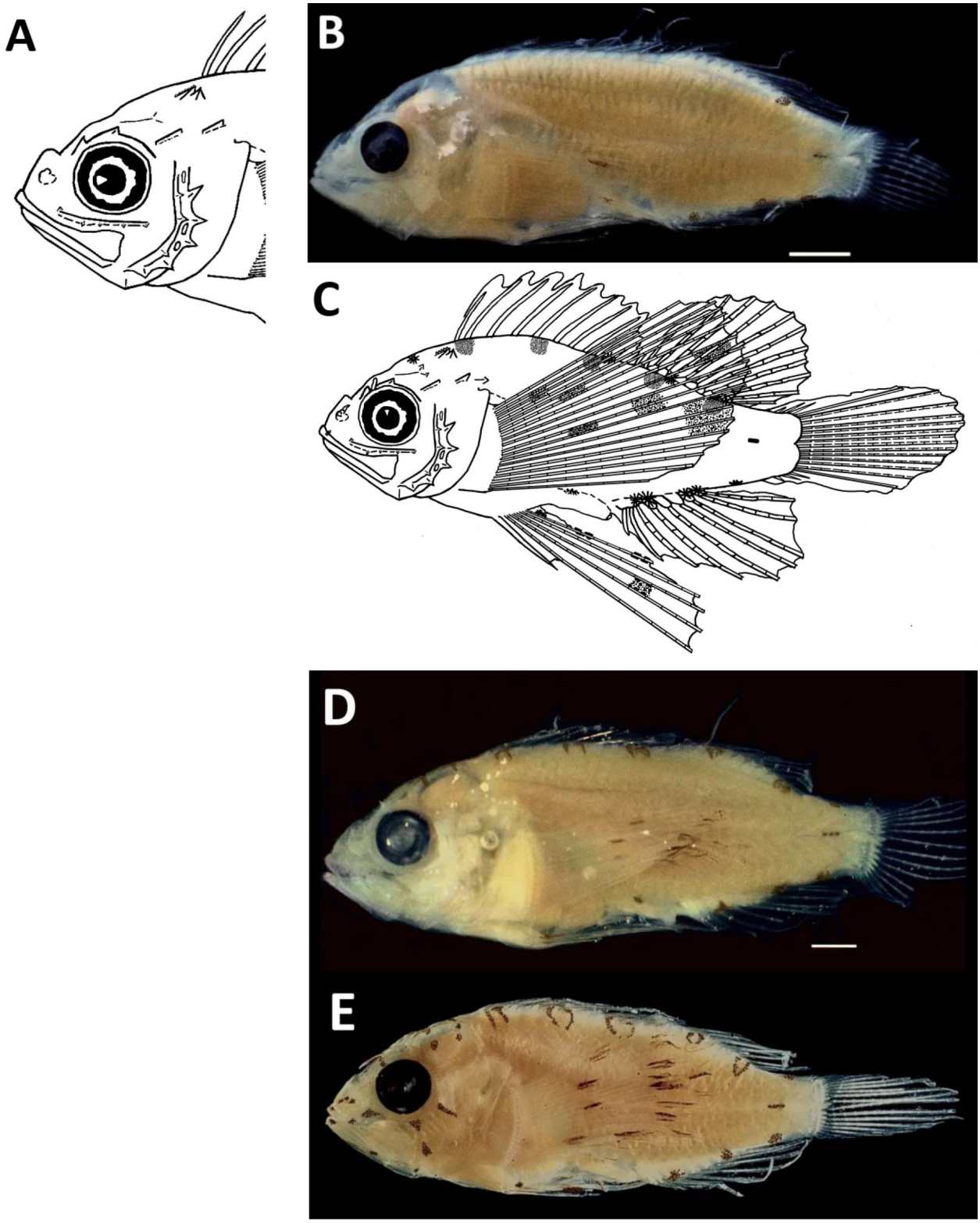

FIGURE 4. *Dendrochirus barberi* larvae. A. cranial & opercular spination at 8.6 mm; B. 9.1 mm; C. 11.0 mm; D. 12.2 mm; E. 14.0 mm. Pigment enhanced in some images for detail purposes. All lengths in mm standard length (SL). Scale bar = 1.0 mm.

Cephalic and opercular spination; supraocular and nasal cirri; and sensory pore development

Smallest larva with five PPO and three APO spines, PPO's subequal, each <35% OD (Fig. 4a). PPO-1 and -2 along upper margin: PPO-1 about mid-orbit, directed dorsoposteriorly; PPO-2 directed posteriorly. PPO-3 through -5 along lower margin: PPO-3 below shelf angle nearly aligned with dorsal margin of maxilla; PPO-4 near lower margin of pectoral-fin base directed posteroventrally; PPO-5 near angle of lower jaw, directed ventrally. APO-1 and -2 along upper margin of shelf, nearly overlay PPO counterparts; APO-3 along lower margin, closer to PPO-4 than -3. Largest transformer with APO-1 closer to PPO-2, and APO-2 between PPO-3 and -4; transformers lack supplemental spine at base of PPO-1 found in juveniles and adults.

Most cranial ridges and spines weakly developed until early transformation. Smallest larva with outer interorbital, supraocular, postocular, pterotic, lower posttemporal, infraorbital, parietal, and nuchal ridges; and parietal and nuchal spines (Fig. 4a). Parietal ridges weakly dentate, terminate at conjoined base of parietal and nuchal spines. Nuchal spines external to parietals, subequal in length, and lie flatter against cranium (i.e., ≤15° above longitudinal axis of head) than in *P. volitans*. Anterior margin of parietals weakly serrate; posterior margin smooth; nuchal margins smooth at all sizes examined. Low, outer interorbital ridges originate above mid-orbit, diverge outward toward posterolateral margin of cranium, connect to coronal base, then bifurcate into low coronal and tympanic ridges. By 11.5 mm, transformers with short, flimsy spine on terminal margin of each ridge lies nearly flat against cranium, best observed by lifting with probe.

Supra- and postocular ridges project outward over eyes like "blinders," each ridge with dorsoposteriorly directed spine in smallest larva. Supraocular ridge rises to acute peak along anterodorsal margin of orbit, descends thereafter to become postocular ridge; postocular ridge rises to acute peak near mid-orbit, descends along posterior margin of orbit; height of both ridges gradually reduced during transformation to become low continuous ridge with scalloped outer margin in largest transformer. Smallest larva with pterotic and lower posttemporal ridges swollen, laterally projecting, increase in height in posterior direction, short terminal spine on each (Fig. 4a). Height of lower posttemporal ridge nearly twice that of pterotic ridge in early transformers; largest transformer with posterior half of pterotic ridge weakly dentate. Transformers add supracleithral ridge by 10.0 mm. Below orbit, smallest larva with low IO ridge, small spine on IO1-U1, IO1-L1, and ventrally near terminal margin of IO4; IO1-L1 overlaps dorsal margin of upper lip in transformers. By 11.0 mm, two small spines added on lateral margin of ridge along IO3, posterior spine slightly larger than anterior spine.

Smallest larva with cephalosensory canal along IO1 and outer margin of PPO. Canal along PPO with single pore above PPO-1, between PPO-2 and -3, and between -3 and -4 (Fig. 4a). Transformers add sensory canal along postocular, pterotic, and lower posttemporal ridges; along lower margin of operculum; and on snout and frontal region of head above nares. By 11.0 mm, transformers with V-shaped tooth patch on vomer, and short cirrus on dorsal rim of anterior nostril, and above eye (i.e., nasal and supraocular cirri; Fig. 4c). Largest transformer with supraocular cirrus >50% OD, well pigmented; tip of unpigmented nasal cirrus extends to about mid-orbit if pressed against forehead. Transformers lack nasal, opercle, interopercle, and subopercle spines; and sphenotic and medial interorbital ridges.

Dendrochirus hemprichi: general morphology

We examined images of two transforming larvae of *D. hemprichi*, one from Baldwin (2013: 540, fig. 40E) labeled *D. brachypterus*, and an 11.0 mm larva from the Red Sea (Fig. 5a–b). These larvae were not available for examination and measurement; therefore, the following description of general morphology applies to the 21.0 mm juvenile only (Fig. 5c). Head length 38% SL; OD about 1.5 times wider than snout. PPO-1 length 25% OD (Table 2), and two times longer than PPO-2 through -5. Upper jaw terminates slightly beyond mid-orbit; maxilla swollen near its posterior margin. Preanal length 67% SL; BDc 43% SL; CP depth 36% BDc; CP length 75% of its depth; maximum width of pectoral-fin base 39% BDc (Table 2). Seven BR.

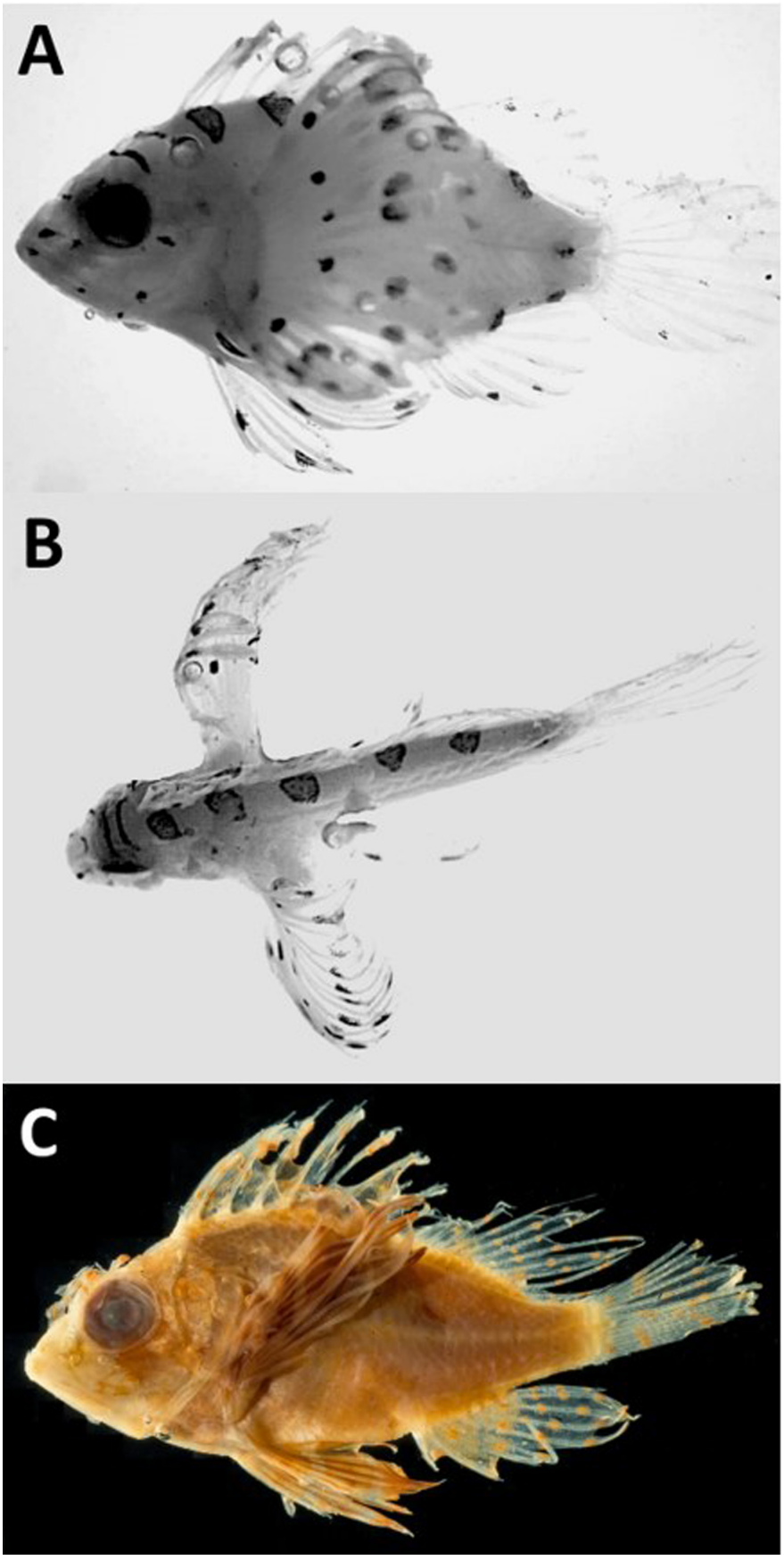

FIGURE 5. *Dendrochirus hemprichi*. A. transforming larva captured in the Red Sea estimated to be about 11.0 mm standard length (SL); B. dorsal view, same larva. C. juvenile *D. hemprichi* (21.0 mm SL) captured off South Sail Rock Channel, Kenya (LACM 31619.017).

Pigmentation

Transformers with pair of narrow stripes across dorsal surface of head: anterior stripe between posterior margin of orbits, posterior stripe between bases of parietal spines; a partial third stripe between lower margin of orbits. Lateral surface of snout with horizontal blotch near nares. Elsewhere, pigment near anterior margin and midway along lateral surface of lower jaw, below anteroventral margin of orbit, and near angle of lower jaw. Cheek with pigment behind posteroventral margin of orbit (Fig. 5a), and diffuse blotch near anterior margin of gas bladder. Five roughly circular "saddles" along dorsal margin of body: anteriormost near origin of spinous dorsal fin, posteriormost near terminal margin of soft dorsal base (Fig. 5a-b). Lateral midline of CP with short series of close-set melanophores. Ventrally, pigment near insertion of pelvic fins, near origin and termination of anal-fin base, and along posterior third of CP (Fig. 5a). Presence or absence, and location of pigment along dorsolateral surface of hindgut uncertain, area concealed by pectoral fins in image (Fig. 5a).

Pectoral- and pelvic-fin pigmentation pronounced in transformers. Pectoral fin with series of roughly circular to oblong blotches in uneven rows near mid-fin and toward its outer margin; single blotch near base of rays 12–13. Pelvic fin with blotch on membrane between spine and outermost ray about halfway between inner and outer margins, another blotch near outer margin of fourth ray, and near origin of fin base. Dorsal fin with pigment on webbing or along shaft of second and third spines, and near outer margin of anterior few rays; anal fin with pigment near outer margin of first and second rays; primary rays of caudal fin with pigment on membrane or along shaft of numerous rays near mid-fin and outer margin (Fig. 5a).

Pigment faded, but juvenile with three bands on lateral surface of head: anterior band near anteroventral margin of orbit down across upper lip; diagonal medial band from supraocular cirrus across eye to posterior margin of interopercle; posterior band from margin of orbit across PPO. Snout with narrow bar or band from rim of lower nostril to dorsal margin of lower lip. Operculum and sides of upper and lower jaws mottled. Abdomen of juvenile with series of faint saddles along dorsal and ventral margins as described for transformers; mid-CP with partial band across dorsal margin. Dorsal and anal fins with series of circular to oblong blotches on shaft and webbing of most elements. Caudal fin with series of pigments in three irregular bands, indication of fourth band near outer margin of existing rays. Pelvic fins with three broad bands of pigment (Fig. 5c). Folding of rays and loss of pigment due to long-term preservation makes pectoral-fin pigmentation pattern uncertain.

Fin development

Transformers with full complement of primary elements in all fins. Spinous and soft dorsal-fin bases continuous, spinous base about three times longer than rayed portion. Tips of most dorsal- and all anal-fin rays extend to or beyond posterior margin of CP. Third element of anal fin transformed into third spine in juvenile (Table 3).

Juvenile with 7+7 primary caudal rays (outermost on each side unsegmented), 3+3 secondary elements (20 total). Gap between first and second dorsal spines narrower than between subsequent spines; second spine about 25% longer than first; spines two through seven similar in length; 12th shortest; 13th about three times longer than 12th. First dorsal pterygiophore inserted above posterior margin of APO. Second spine of anal fin two times longer than first (Table 2); third spine slightly longer than second. Pterygiophore of first anal spine inserted below 12th dorsal spine; first "true" ray of anal fin inserted below first to second pterygiophore of soft dorsal-fin base; terminal pterygiophore of anal-fin base inserted below sixth to seventh pterygiophore of soft dorsal-fin base. Tips of dorsal and anal rays initially bifurcate, not those in pectoral and pelvic fins. Juvenile with pectoral fins relatively shorter than in transformers, tips of longest rays extend to, but not beyond, terminal margin of dorsal-fin base. Tips of longest pelvic rays extend to third anal spine; tip of pelvic spine short of anus when pressed against body. Membrane attaches innermost pelvic ray to abdominal wall for about 40% of its length. Terminal ray of dorsal fin attached by membrane to body wall for about 15% of its length; terminal ray of anal fin free from body.

Cephalic and opercular spination, and cephalosensory canals

Images of transformers reveal supraocular, postocular, parietal, and nuchal ridges, each with spine. Pterotic and posttemporal ridges also present, and small spine on IO1-L1 and IO2-L1. Unable to determine presence or absence

of cephalosensory canals or details of PPO spination from images, but 9.2 mm larva in Matsunuma *et al*. (2017) has five spines.

Description below applies to juvenile only. Spines along APO subdermal or resorbed. Five PPO's, upper three exposed, lower two subdermal. PPO-1 and -2 along upper margin; PPO-3 slightly below shelf angle; PPO-4 and -5 along lower margin. PPO-1 nearly aligned with lower rim of orbit, oriented slightly upward, its length about 25% OD. PPO-1 nearly two times longer than PPO-2 and -3, small supplemental spine at base of PPO-1. PPO-2 oriented slightly outward from axis of head, similar in length to PPO-3, but more acute; PPO-3 directed posteriorly. Opercle, interopercle, and subopercle lack spines. Cephalosensory canals and pores obscured by epithelium in juvenile, but series of three-tubed scales along trunk lateral line immediately behind head. Numerous scales and scale pockets on shoulder, abdomen, and CP suggest scale development complete or nearly so by 21.0 mm.

Juvenile with most cranial ridges and spines low, subdermal. Parietal ridge terminates in short, dorsoposteriorly directed parietal and nuchal spines, elevation ≤15° above longitudinal axis of head; nuchal spine attached to outer margin of parietal base, nuchals behind, slightly smaller than parietals. Pterotic and lower posttemporal ridges laterally swollen, both terminate in small spine. Lower posttemporal ridge elevated posteriorly, higher, but shorter, than pterotic ridge. Supraocular ridge smooth, postocular ridge rises to low, obtuse lateral peak near mid-orbit, descends along posterior rim. Entire IO ridge elevated, lateral margin smooth, slight indentation between IO1 and IO2. Spine on IO1-L1 overlaps dorsal margin of upper lip. Coronal and tympanic ridges elevated, tympanic ridge two times higher and longer than coronal; lacks medial interorbital ridge. Vertical pair of short, parallel, weakly dentate sphenotic ridges behind orbit. Elevated supracleithral ridge terminates in short spine.

Dermal flaps, and supraocular and nasal cirri

Transformers with short supraocular and nasal cirri; nasal cirrus along dorsal rim of anterior nostril. Juvenile with supraocular cirrus about 85% OD, and encircled by three bands; tip spade-shaped. Nasal cirrus slender, encircled by narrow band about mid-length, tip extends beyond mid-orbit if pressed against forehead. Juvenile with pair of filamentous barbels just above upper lip, barbels shorter than nasal cirrus. Small pigmented flap on anterodorsal surface of eye, and minute flap on anteroventral margin of IO1–L1. Leafy flap behind IO2-L1 with many bands, margin double-toothed; another flap along posteroventral margin of PPO adjacent to lowermost ray of pectoral fin. Location, presence or absence, size, and shape of dermal flaps and snout barbels difficult to determine without stain.

Dendrochirus "bellus" and *D. zebra*

General morphology and pigmentation patterns for transforming *D*. "*bellus*" and *D*. *zebra* similar to that described for *D*. *barberi* and *D*. *hemprichi*. Per Kojima (2014), 9.5 mm *D*. "*bellus*" with large eyes, maximum body depth 38% SL; HL 36% SL. Hindgut long, relatively slender. PPO spines relatively short; pterotic and posttemporal ridges elevated posteriorly. Parietal spines anterior to nuchals, subequal in length, relatively short. Supraocular cirrus pigmented; nasal cirrus unpigmented. Dorsal and anal spines slender; first eight dorsal spines of similar length. Pectoral fins fan-shaped, rays elongate (Fig. 6a). Three stripes across dorsal surface of head: anteriorly between orbital margins, midway between pterotic ridges, and posteriorly near base of parietal spines. Snout with narrow swath from lower nares downward onto upper lip, and from anteroventral margin of orbit across IO1. Pigment near anterior margin and on posterolateral surface of lower lip; diffuse blotch near angle of lower jaw. Cheek with narrow diagonal swath from dorsoposterior margin of maxilla across lower part of APO, and another from posterior margin of orbit across APO; opercle with diffuse, oblong swath (Fig. 6a). Lateral surface of visceral mass unpigmented. Internally, dorsal surface of gas bladder lightly pigmented; hindgut with pigment midway along dorsolateral surface (partially obscured by pectorals in illustration; Fig. 6a). Body with five partial saddles or elongate dorsolateral bands. Ventrally, "circular" pigment on abdomen near origin of pelvic fins, and diffuse blotch on pterygiophores 3–4 and terminal pterygiophore of anal-fin base; also, a diffuse vertical swath from ventral margin to lateral midline near mid-CP. Pectoral fins with diffuse blotch on shaft and membrane near insertion of rays 11–13, a series of blotches in two uneven rows (near mid-fin and toward outer margin), and pigment scattered along outer margin of fin; webbing

weakly incised (Fig. 6a). Pelvic fins damaged, but comparably developed 9.2 mm larva with tips of middle rays beyond origin of anal-fin base (Kojima 2014). Caudal-fin outer margin rounded.

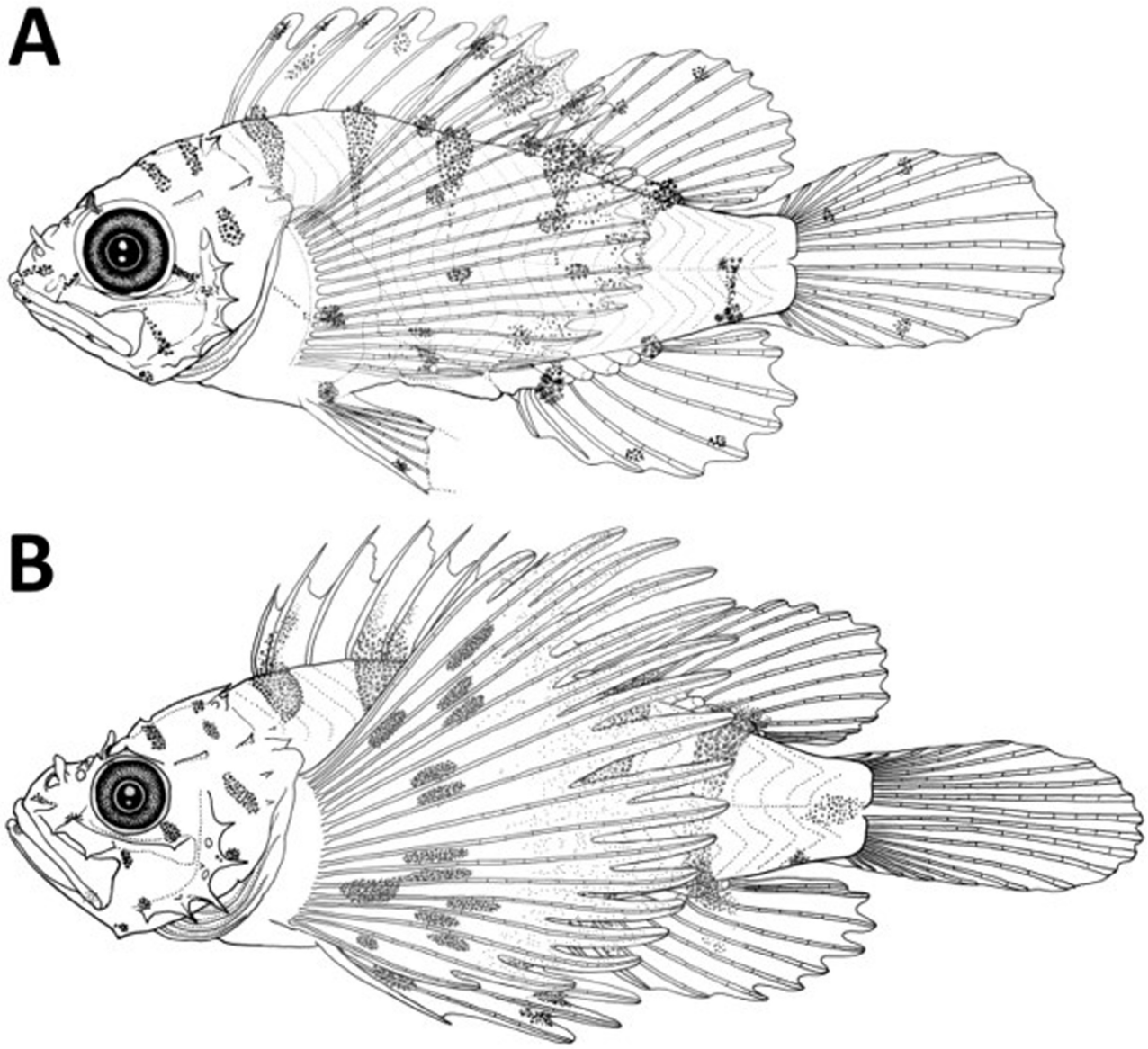

FIGURE 6. A. transforming 9.5 mm standard length (SL) *Dendrochirus* "*bellus";* B. 11.5 mm SL *D. zebra* from Kojima (2014) used by permission of author and publisher.

Additional characteristics we observed in Kojima's (2014) *D.* "*bellus*" include small cluster of melanophores on upper margin of orbital membrane adjacent to base of supraocular cirrus. Upper four PPO spines subequal in length, lowermost shortest; cephalosensory canal with pore above PPO-1. Parietal and nuchal spines dorsoposteriorly directed, elevation ≤15° above longitudinal axis of head. Supracleithral ridge with terminal spine. Spine on IO1–L1 slightly overlaps upper margin of maxilla. Image of larger cleared and stained larva provided by Kojima (pers. comm.) reveals low supraocular and postocular ridges with short spine along each, and short, blunt spine along posteroventral margin of IO4. First and second dorsal spines of similar length, gap between these spines narrower than subsequent spines. Length of first anal spine about two-thirds that of second; third element of anal fin ray-like, untransformed. Pelvic spine short of anus; pigment on membrane between pelvic spine and outermost ray. Clusters of melanophores near tip of first three dorsal spines, on membrane between spines 2–3 and 4–5, and at various locations along shaft or on membrane of dorsal, anal, and primary caudal rays. Series of melanophores along longitudinal axis of pectoral-fin base (not on surface of visceral mass; Kojima, pers. comm.).

Per Kojima (2014), 11.5 mm *D. zebra* with eyes relatively smaller than in *D.* "*bellus*," maximum body depth 33% SL; HL about 34% SL; nasal and supraocular cirri relatively short. Five PPO spines; cephalosensory canal

along shelf with pore between PPO-1 and -2, and -3 and -4. All fins well developed; second dorsal spine about 30% longer than first. Pectoral fins elongate, fan-shaped, webbing between rays well incised; tips of longest rays short of terminal margin of dorsal-fin base. Pectorals also have a series of diffuse, elongate blotches in uneven row across inner half of fin; outer half peppered with melanophores. Tips of longest rays of pelvic fin extend to about middle of anal-fin base; dusky, teardrop shaped blotch on inner third of shaft and membrane of outer two rays; clusters of pigment on webbing near outer margin between most rays (Fig. 6b). Head pigmentation similar to that of *D*. "*bellus*" with addition of pigment cluster on cheek adjacent to PPO-2. Five dorsolateral bands or saddles of comparable width extend onto spinous- and soft-dorsal fins; posterior pair of bands extends onto anal fin. Ventrally, abdomen with small cluster above insertion of pelvic fins (not visible in lateral view); CP with diffuse ventrolateral cluster near mid-peduncle, and roughly diamond-shaped lateral cluster in hypural area. Light cluster of pigments on dorsolateral surface of hindgut near anus partially obscured by pectoral fins in illustration. Caudal-fin outer margin rounded.

Additional characteristics we observed in Kojima's (2014) illustration of *D. zebra* include small cluster of melanophores on upper margin of orbital membrane adjacent to base of supraocular cirrus as noted for *D*. "*bellus*". OD nearly equal to snout length. Upper four PPO spines subequal, lowermost shortest; two small APO spines, uppermost inserted between PPO-2 and -3, lowermost overlays PPO-4. PPO spines somewhat longer in *D. zebra* than in *D. barberi* and *D*. "*bellus*," but placement and orientation similar in all three. Pterotic and posttemporal ridges elevated posteriorly, pterotic ridge longer, but lower, than lower posttemporal. Lower posttemporal ridge with acute terminal margin; small spine on upper posttemporal ridge. Parietal spines anterior to nuchals, subequal in length, relatively short and dorsoposteriorly directed, elevation ≤15° above longitudinal axis of head. Supraocular and postocular spines along orbit. Nasal spine above posterior nostril; nasal and supraocular cirri of similar length, supraocular cirrus partially pigmented. Tip of IO1-L1 and IO2-L1 slightly overlap upper margin of maxilla; short spine along lower margin of IO4. Pair of acute "spine-like" structures or short ridges near margin of opercle (Fig. 6b). Gap between first and second dorsal spines narrower than between subsequent spines. Second dorsal spine about 25% longer than first; second anal spine about two times longer than first. Third element of anal fin ray-like, untransformed; tip of pelvic spine short of anus. Caudal fin unpigmented.

Juvenile *D. zebra* <15.0 mm in Matsunuma & Motomura (2019) have three, long snout barbels; nasal cirrus, very long, branched; supraocular cirrus long, unbranched; head lacks obvious dermal flaps. Upper three PPO spines exposed (lower two perhaps subdermal, or resorbed); PPO-1 longest, PPO-2 and -3 of similar length, all lack supplemental spines. Single nasal spine. These juveniles also lack sphenotic, pterotic, lower posttemporal, supracleithral, coronal, tympanic, postorbital, and opercular spines. Therefore, pterotic, lower posttemporal, and supracleithral spines in 11.5 mm transformer either subdermal, or resorbed, by 15.0 mm. Infraorbital ridges smooth, small IO1-L1; IO1-L2 flat, plate-like. Conspicuous oblique band crosses eye from base of supraocular cirrus to interopercle; otherwise, head, body, and pectoral- and pelvic fin pigmentation as described for 11.5 mm *D. zebra* (Kojima 2014). Light, downward curved swath from lateral midline to ventral margin of CP (i.e., sixth band) in a 14.0 mm larva examined by Matsunuma & Motomura (2019) corresponds to diamond-shaped, mid-lateral cluster in Fig. 6b. Numerous poorly defined, elongate blotches added to rayed portions of dorsal, anal, and caudal fins in early juveniles.

Trachyscorpia cristulata and *Phenacoscorpius nebris*

Early life stages of deep-water members of *Idiastion kyphos* Eschmeyer, 1965, *Neomerinthe* spp., *Phenacoscorpius nebris* Eschmeyer, 1965 (Scorpaeninae), *Setarches guentheri* Johnson, 1862 (Setarchinae), and *Trachyscorpia cristulata* (Goode & Bean, 1896) (Sebastolobinae), included in Sebastinae by Hardy (2005), have not been described, to our knowledge. While a visiting scientist at the Smithsonian Institution (NMNH), the senior author examined the smallest available specimen of *T. cristulata* (32.0 mm SL; USNM 72979; collected 14 February 1902 off Key West, Florida) and *P. nebris* (40.0 mm SL; USNM 422671; collected 24 May 2013 off Curacao); small juveniles of the other aforementioned taxa were not available in NMNH collections for examination. Our intent was to generate a suite of characteristics to enable recognition and discrimination of late postflexion and transforming larvae of *T. cristulata* and *P. nebris* from other scorpaenids in the WNA.

Trachyscorpia cristulata with cranial spines strongly developed. Elevated parietal ridge terminates in longer nuchal than parietal spines; parietals behind nuchals. Opercle with pair of ridges or struts, upper ridge directed

dorsoposteriorly, lower ridge directed posteriorly, short spine at outer margin of each. Pair of spines on IO1 overlap dorsal margin of maxilla, and series of eight laterally projecting spines of varying length along remainder of IO ridge. Other ridges and spines are as described by Ginsburg (1953) and Eschmeyer (1969), and include preorbital (i.e., IO1), supraocular, postocular, nasal, tympanic, pterotic, sphenotic, lower posttemporal, supracleithral, and cleithral; juvenile lacks upper posttemporal spine. PPO-1 longest, aligned with IO ridge, spine directed dorsoposteriorly; length of supplemental spine at its base about one-third that of PPO-1; PPO-1 about two times longer than PPO-2; PPO-2 through -4 similar in length, PPO-5 shortest. Length of supraocular cirrus about one-third OD. Ocular surface with ring of papillae; longer on anterior than posterior half of eye.

Dorsal-fin count XII, 9; spines increase in length from first to third, progressively shorter thereafter; penultimate spine about one-third that of terminal spine. Anal-fin count III, 5; length of first anal spine about 35% of second; second and third subequal, second notably thicker than third. Pectoral-fin ray count 23, fin length uncertain, rays broken on both sides of body; however, fins typically extend to or just short of anus in juveniles, with longest rays toward upper part of fin (Ginsburg 1953; Eschmeyer 1969). About 30% of innermost pelvic ray attached by membrane to abdomen, based on ray length. Tips of longest pelvic rays extend to anus in specimen examined, but well short of anus in adults (Ginsburg 1953; Eschmeyer 1969). Lateral line extends to base of caudal fin; middle primary caudal rays longer than those toward outer margins. Lacks small slit behind fourth gill arch. Body and fin pigmentation pattern difficult to assess due to long-term preservation; however, head and body peppered with melanophores of various sizes similar to that of juvenile sebastolobines from eastern Pacific (see Moser 1996).

Phenacoscorpius nebris with cranial spines strongly developed. Parietal and nuchal spines conjoined at base, parietals anterior to and longer than nuchals. Opercle with pair of ridges or struts, upper ridge directed dorsoposteriorly, lower ridge directed posteriorly, short spine at outer margin of each. Pair of spines on IO1 (i.e., preorbital of Eschmeyer 1965) overlap dorsal margin of maxilla, and ridge behind IO1 has five relatively stout, laterally projecting spines (i.e., suborbital and postorbital series of Eschmeyer 1965). Other spines as described by Eschmeyer (1965, 1969) include nasal, preocular, supraocular, postocular, tympanic, pterotic, upper and lower posttemporal, supracleithral, and cleithral.

Length of PPO spines differs between left and right sides of head. PPO-1 longest on left side, aligned with IO ridge, length of supplemental spine at its base about one-half that of PPO-1; PPO-2 blunt, "knob-like," considered absent by Eschmeyer (1965); length of PPO-3 about one-half that of PPO-1; PPO-4 and -5 progressively shorter, lowermost covered by epithelium. PPO-1 and supplemental spine on right side as described above for left side, but PPO-2 longer than -1; PPO-3 blunt, "knob-like," resembles PPO-2 on left side; PPO-4 and -5 progressively shorter, blunt. Supraocular cirrus short, multifurcate. Three-row arc of short papillae on surface of anterior half of eye; small flap on upper anterior and lower posterior margins of orbit. Small cirrus along IO1; small pigmented flap on ventral margin of lower nostril.

Dorsal-fin count XII, 9; spines increase in length from first to third, gradually decrease thereafter, penultimate spine about one-half that of terminal spine. Anal-fin count III, 5; second anal spine thicker, 20% longer than third. Pectoral-fin ray count 16, fins placed low on body just above and slightly behind pelvic fins. Melanophores pepper base and inner third of pectoral-fin rays; fins also have two narrow "bands" of pigment near mid-fin. All pectoral rays extend to or slightly beyond anus, with tips of rays 9 through 11 beyond first anal spine. About 50% of innermost pelvic ray attached by membrane to abdomen based on ray length, middle three rays longer than innermost and outermost, all rays well short of anal-fin base. Lateral line incomplete, 3–4 tubed scales immediately behind head. Small slit present behind fourth gill arch.

Body and fin pigmentation as described for a 29.3 mm *Phenacoscorpius megalops* Fowler, 1938 (listed as *P. nebris* in Eschmeyer & Randall 1975: fig. 11). Saddle of pigment near dorsal-fin origin, dark blotch on membrane between fifth and ninth dorsal spines, and dusky band between soft dorsal and anal fins that extends onto associated bases and inner half of rays; also, a band of pigment on CP at base of caudal fin composed of large melanophores. All areas of head peppered with melanophores, including membrane surrounding orbit and lower surface of iris; visceral mass with scattered blotches of pigment.

Discussion

Pterois volitans larvae from the Gulf of Mexico differ from those described as *P. volitans* by Imamura & Yabe (1996) in pigmentation, cephalic spination, and OD to snout length ratio. Larvae from the Gulf of Mexico have a series

of melanophores or streak of pigment along the dorsal, lateral, and ventral midlines on the posterior third of the body at at all sizes; flexion larvae add pigment internally on the lobes of the mid- and hindbrain, above the first few precaudal vertebrae, and along the dorsoposterior margin of the hindgut; and early postflexion larvae add pigment on the dorsal and lateral surfaces of the hindbrain (Kitchens *et al.* 2017; this study). By comparison, the 3.8 mm and 4.5 mm larvae from the eastern Indian Ocean have only two small melanophores along the posteroventral margin of the CP, and lack pigment elsewhere along the body midlines; larvae also lack pigment internally on the surface of the hindgut and on the lobes of the mid- and hindbrain at all sizes (Imamura & Yabe 1996). In addition, Imamura & Yabe (1996) described the 4.5 mm larva as having a "third posterior opercular spine [sic] with serrations," possibly our PPO-3, and "blunt upper opercular spine [sic]," possibly PPO-1. The 9.5 mm larva has a "tympanic spine," and adds "two lower opercular spines [sic] by 11.0 mm SL," possibly PPO-4 and -5. Larvae from the Gulf of Mexico, however, lack a tympanic spine, as do adults of *P. volitans* (Yoshida *et al.* 2013); have a full complement of four APO and four PPO spines by 7.0 mm, and only our 12.9 mm larva has the margin of the upper three PPO spines weakly serrate. *Pterois volitans* larvae from the Gulf of Mexico also have a larger eye (i.e., OD 10–15% greater than snout length) than those from the eastern Indian Ocean (i.e., mean snout length exceeds OD by 18%). If the "two lower opercular spines" are PPO spines, a likely scenario given that juveniles and adults of all members of *Pterois* (e.g., Matsunuma & Motomura 2016a) lack spines on the opercle, then the larvae Imamura & Yabe (1996) describe have five PPO's, not four, as in our *P. volitans*.

Imamura & Yabe (1996) exclude other lionfishes found off northwest Australia as potential candidates based on species distributions and meristics for taxa known at that time. Whereas differences in either total dorsal-, anal-, or pectoral-fin ray counts exclude members of other pteroine genera (Table 4), the true identity of the larvae described cannot be determined with certainty because *P. andover* Allen & Erdmann, 2008, *P. miles*, and *P. russelii* also have 13–14 pectoral-fin rays, and co-occur, or potentially co-occur, with *P. volitans* off northwest Australia (Tables 1 & 4). *Pterois andover*, however, can likely be excluded as a candidate due to its rarity and restricted distribution (Table 1). One reviewer suggested that based on spatial distributions off northwest Australia, the identity of Imamura & Yabe's (1996) larvae may be *P. miles*. Branchiostegal-ray count may have resolved the identity had that information been available because all members of *Pterois* have seven, except *P. russelii* with six (Matsunuma *et al.* 2016).

Members of *Pterois* typically have 12–13 (rarely <12) dorsal spines (Table 4), which makes our 12.9 mm *P. volitans* with nine unique (Fig. 2g). Specimen capture information places the collection site southwest of the Macondo DWH wellhead (28°44′17″N, 88°21′58″ W), which released 780,000 m^3 of crude oil into the northeastern Gulf of Mexico between April and September of 2010 (McNutt *et al.* 2012). Two years later, about 50% of the oil originally released remained in subsurface waters (McNutt *et al.* 2012) with seawater samples taken at least 100–200 km from the wellhead exceeding toxicity thresholds for crude oil-derived polycyclic aromatic hydrocarbons (PAH) (Adcroft *et al.* 2010; Incardona *et al.* 2014). ELS of fishes exposed to mixtures of PAH's and the chemical dispersants used to dissipate the oil exhibited higher rates of mortality, and developed abnormalities specific to crude oil exposure, such as lack of actinotrichia development and reduced finfold growth (Incardona *et al.* 2014). Based on regional ocean current patterns, specimen collection date (01 Sept. 2011) and location, and a mean pelagic duration of 26–30 days for *P. volitans* (range: 20–39 days; Ahrenholz & Morris 2010; Côté & Green 2012), exposure to mutagenic concentrations of PAH's from the DWH oil spill event during early development may have disrupted actinotrichia development in the 12.9 mm larva, a hypothesis consistent with the findings of Incardona *et al.* (2014) and the abnormally low number of dorsal spines and associated structures (Fig. 2g), although there may be other explanations.

Differences in cranial spination and pigmentation patterns separate *P. volitans* from larvae of the four members of *Dendrochirus*. *Pterois volitans* has parietal spines two or more times longer than the nuchals, with both sets of spines oriented about 30° above the longitudinal axis of the head, whereas larvae of the four members of *Dendrochirus* have relatively short, low parietal and nuchal spines subequal in length that lay flatter against the cranium (i.e., elevation ≤15° above longitudinal axis of head). Given that low parietal spines unite members of *Dendrochirus* (Eschmeyer & Randall 1975; Matsunuma *et al.* 2017), if larvae of other members of *Pterois* possess the parietal and nuchal spine pattern described for *P. volitans*, differences in relative length and elevation of these spines discriminate larvae of the two genera. Larvae of the four members of *Dendrochirus* also develop "saddles" of pigment along the dorsal and ventral margins of the body during transformation that *P. volitans* and the *Pterois* sp. described by Imamura & Yabe (1996) lack at the sizes described. In addition, members of *Dendrochirus* typically have fewer total anal-fin elements (i.e., ≤8) than those of *Pterois*, which have ≥9 (Table 4).

Eschmeyer & Randall (1975) suggested that differences in pectoral-fin length, and the presence of branched rays in *Dendrochirus* spp., and lack thereof in *Pterois* spp., distinguish members of these two taxa. Fin length, however, is not a reliable character to discriminate larvae because rays are often broken off in the ELS during specimen collection and handling, and the pectoral fins become relatively shorter with growth in members of both genera (Matsunuma & Motomura 2016a; Matsunuma *et al.* 2017). Moreover, the presence or absence of branched rays in the pectoral fin does not distinguish larvae and small juveniles of these taxa because rays do not branch in *Dendrochirus* spp. until ≥40 mm SL (Matsunuma *et al.* 2017), a trend common to most pteroine (Matsunuma & Motomura 2015a, 2019) and non-pteroine scorpaenid genera.

Differences in meristics (Table 4) and pelvic-fin pigmentation pattern distinguish larvae of one or more members of the four *Dendrochirus*. *Dendrochirus barberi* has pigment on the inner third of the membrane that connects the innermost pelvic ray to the abdominal wall; *D. hemprichi* and *D.* "*bellus*" have pigment between the pelvic spine and outermost ray; and *D. zebra* has a dusky, teardrop-shaped blotch on the inner third of the shaft and membrane of the outer two rays. Although the number and length of snout barbels (Table 4), and number and placement of dermal flaps on the head can also help distinguish some members of *Dendrochirus*, these characters may not develop until the juvenile life phase, based on their absence in transforming larvae of the four members of *Dendrochirus*, and presence thereof in the juvenile *D. hemprichi*.

The length of transforming larvae and literature reports of the largest presettlement larvae and smallest documented settlers suggest that several members of *Pterois* and *Dendrochirus* settle between 12.0–15.0 mm SL: the three largest plankton-collected *P. volitans* (e.g., 14.2 mm, Sponaugle *et al*. 2019; 15.0 mm & 15.3 mm, Mostowy *et al.* 2020) and smallest recent settler (13.0 mm, Byron *et al.* 2014) collected in the Gulf of Mexico; the image of a 15.5 mm *P. volitans* in Motomura & Matsuura (2014), which displays the characteristics of an early juvenile; images of a 13.0 mm recently settled *P. radiata* (Cuvier in Cuvier & Valenciennes, 1829) in Lo-Yat (1998) and 14.6 mm early juvenile in Motomura & Matsuura (2014); the mixed assemblage of recently settled lionfishes observed in the Red Sea estimated by Fishelson (1975) to be 10.0–12.0 mm SL, and likely to include *P. miles* and *P. cincta* Rüppell, 1838; and recently settled *P. antennata* (Bloch, 1787) (15.0 mm total length [TL]) collected off French Polynesia in Maamaatuaiahutapu *et al.* (2006). Likewise, similar records for members of *Dendrochirus* are consistent with settlement between 12.0–15.0 mm SL*:* our largest transforming *D. barberi* (14.0 mm) and the smallest settler (16.3 mm, USNM 442423, photo by Diane E. Pitassy, USNM); the 10.0 mm and 11.0 mm transforming *D. hemprichi* described here, and the mixed assemblage of small, recently settled lionfishes observed in the Red Sea, and likely to include *D. hemprichi* in Fishelson (1975); the 9.5 mm transforming *D.* "*bellus*" (Kojima 2014); and the 11.5 mm transforming (Kojima 2014) and 14.0 mm juvenile *D. zebra* (Matsunuma & Motomura 2019).

Although the ELS of members of *Brachypterois*, *Ebosia*, and *Parapterois* have not been described, most scorpaenids have the full complement of cranial and opercular spines possessed by juveniles and adults before or during transformation (except some species of *Sebastes*; Moser 1996). Therefore, differences in cranial and opercular spination patterns may permit recognition and identification of late postflexion and transforming larvae of members of these three pteroine genera, and reveal characteristics that discriminate their ELS from those of *Dendrochirus* and *Pterois*. For example, larvae of *P. volitans*, *D. barberi*, *D. hemprichi*, and *D.* "*bellus*" lack spines on the opercle, as do juveniles and adults of all members of *Dendrochirus* and *Pterois* (e.g., Matsunuma & Motomura 2016a; Matsunuma *et al*. 2017). Juvenile members of *Ebosia*, however, have a spine along the upper margin of the opercle (Matsunuma & Motomura 2015a, 2016b), and those of *Parapterois* have a spine along the lower margin of the opercle (Matsunuma & Motomura 2022). Members of *Brachypterois* have a spine on the upper margin, like those of *Ebosia*, and may or may not have a spine (typically subdermal, if present) on the lower margin (Matsunuma *et al.* 2013). The "spine-like" structures near the outer margin of the opercle that we noted in Kojima's (2014) illustration of a 11.5 mm *D. zebra* (Fig. 6b), if "spines," are resorbed during transformation because 14.0–15.0 mm *D. zebra* lack said spines (Matsunuma & Motomura 2019). Alternately, these "spine-like" structures may represent the small, thin, flattened "strut" possessed by *D. zebra* (Matsunuma *et al*. 2017). The presence or absence of nuchal spines can also be used to distinguish some pteroine genera. As previously noted, postflexion and transforming larvae of *P. volitans* and the four *Dendrochirus* possess nuchal spines, as do juveniles of members of *Parapterois*, whereas juveniles of *Brachypterois* and *Ebosia* lack nuchal spines (Matsunuma *et al*. 2013; Matsunuma & Motomura 2015a, 2016b, 2022). Whether larvae of members of *Brachypterois* and *Ebosia* have nuchal spines that are resorbed during transformation remains uncertain.

TABLE 4. Meristics for currently valid species of the Indo-Pacific lionfishes (Teleostei: Scorpaenidae, Pteroinae). Range or rare counts in parentheses. *Pterois lunulata* Temminck & Schlegel, 1843 synonymized as *P. russelii* Bennett, 1831 per Wilcox *et al*. (2018). NA: information not available.

Taxon	Dorsal	Anal	Pectoral	Total caudal elements	Snout barbels	References
Brachypterois						
B. curvispina	XIII (XII–XIV), 10 (8–11)	III, 5	15 (14–16)	20	0	Matsunuma *et al*. (2013)
B. serrulata	XIII (XII–XIV), 10 (9–11)	III, 5 (4–6)	15 (14–16)	20	0	Matsunuma *et al*. (2013)
B. serrulifer	XIII (XII–XIII), 10 (9–11)	III, 5 (4)	16 (15–17)	20	0	Matsunuma *et al*. (2013)
Dendrochirus						
D. barberi	XIII, 9 (8–10)	III, 5	18 (17)	20	0–2, short	Eschmeyer & Randall (1975); Matsunuma *et al*. (2017)
D. bellus	XIII, 9 (8–10)	III, 5	17 (16–18)	20	2	Matsunuma *et al*. (2017)
D. biocellatus	XIV, 8	III, 5	20	20	2	Fowler (1938)
D. brachypterus	XIII, 9 (8–10)	III, 5 (6)	17 (16–18)	20	2	Matsunuma *et al*. (2017)
D. hemprichi	XIII, 9 (8)	III, 5	17 (16–18)	20	2	Matsunuma *et al*. (2017)
D. koyo	XIII, 10	III, 7	18	21	3, short	Matsunuma & Motomura (2019)
D. tuamotuensis	XIII, 9	III, 5	19	20	0	Matsunuma & Motomura (2013a)
D. zebra	XIII, 10 (9–11)	III, 6 (5–7)	17 (16–18)	21	3, long	Matsunuma & Motomura (2019)
Ebosia						
E. bleekeri	XIII, 9 (8–10)	III, 7	16 (15–17)	16	0	Eschmeyer & Rama-Rao (1978); Matsunuma & Motomura (2015a)
E. falcata	(XII) XIII, 9 (10)	III, 8 (7)	17 (16–18)	16	0	Matsunuma & Motomura (2015a); Matsunuma & Motomura (2016b)
E. saya	XIII, 9 (10)	III, 8 (7)	17 (18)	16	2, minute	Matsunuma & Motomura (2015a)
E. vespertina	XIII, 9	III, 8 (7)	18 (17)	16	2, minute	Matsunuma & Motomura (2016b)
Parapterois						
P. heterura	XIII, 9 (8–10)	II, 7 (6–8)	19 (18–20)	20–22	0	Matsunuma & Motomura (2022)
P. macrura	XIII, 9 (8)	II, 7	19–20	20–22	0	Matsunuma & Motomura (2022)
P. nigripinnis	XIII, 9	II, 7	19–20	20–22	0	Matsunuma & Motomura (2022)
Pterois						
P. andover	XIII, 11	III, 7	13 (12–14)	22	2	Allen & Erdmann (2008)

.....*Continued on the next page*

TABLE 4. (Continued)

Taxon	Dorsal	Anal	Pectoral	Total caudal elements	Snout barbels	References
P. antennata	XII, 11 (10–12)	III, 6	17 (16)	20	3	Matsunuma & Motomura (2011); Matsunuma & Motomura (2018)
P. brevipectoralis [1]	XIII, 10 (9)	III, 6	15–16	18	3	Mandrytsa (2002); Matsunuma & Motomura (2013b)
P. cincta	XII, 11 (10–12)	III, 6 (7)	16 (15–17)	20	3	Matsunuma & Motomura (2016a); Matsunuma *et al*. (2016)
P. miles	(XII) XIII, 10 (9–11)	III, (5) 6	14 (13)	NA	3	Schultz (1986); Matsunuma *et al*. (2016)
P. mombasae [2]	XIII, 10 (11)	III, 6	18–19 (20)	NA	3	Smith (1957); Matsunuma & Motomura (2015b)
P. paucispinula [2]	XIII, 10 (11)	III, 6	18 (17-19)	20 (21)	3	Matsunuma & Motomura (2015b)
P. radiata	XII, 11 (10–12)	III, 6	16–17	19–20	3	Matsunuma & Motomura (2016a)
P. russelii [3]	XIII, 11 (10–12)	III, 7 (6–8)	13 (12–14)	NA	2	Schultz (1986); Matsunuma *et al*. (2016)
P. sphex	XIII, 10 (11)	III, 6	16 (15)	NA	3	Eschmeyer & Randall (1975); Matsunuma & Motomura (2015b)
P. volitans	(XII) XIII, 11 (10–12)	III, 7 (6–8)	14	22 [4]	3	Schultz (1986)

[1] Dorsal: XIII, 11; Anal: III, 7 in Mandrytsa (2002)

[2] *Pterois mombasae* in Matsunuma & Motomura (2011) should correctly be *P. paucispinula* per Matsunuma & Motomura (2015b)

[3] Only species with six branchiostegal rays; all others have seven

[4] Total caudal-fin elements in largest larva examined

Differences in meristics (Table 4) and general morphology also distinguish some pteroine genera. Members of *Parapterois* typically have more pectoral-fin rays (19–20) and a steep anterodorsal profile with eyes set high and laterally on the head (Matsunuma & Motomura 2022); those of *Ebosia* have more total anal-fin (10–11) and fewer caudal-fin elements (16 total; Table 4); and members of *Brachypterois* have finely serrate ridges rather than distinct spines along the PPO, and spinous ridges along the mandible that other pteroine genera lack (e.g., Kanayama & Amaoka 1981; Matsunuma *et al.* 2013). *Brachypterois* spp. also have short dorsal spines of nearly uniform height connected by a low membrane, and fewer pectoral rays (15–16) than other pteroines, except some members of *Pterois* (Table 4).

Comparison of pteroine scorpaenids, non-pteroine scorpaenids, and morphologically similar taxa

Most scorpaenids differ from other scorpaeniform fishes by having one or two spines along the margin of the opercle, three to five spines along the PPO, a series of IO spines along the cheek, distinct cranial ridges and spines, and a different combination of total elements in the median and paired fins (Moser 1996; Hardy 2005). Although larvae of most non-pteroine scorpaenids are recognizable by some combination of the above characteristics and by their precocious pectoral fins with dark pigment on some portion to most of the fin (Fahay 2007), identification to subfamily or lower has remained problematic because ELS of most taxa are undescribed or inadequately described, and characteristics that define genera are poorly understood (Moser *et al*. 1977), a problem made more difficult by introduction of the non-native *P. volitans* and *P. miles* into the WNA. Likewise, some characteristics important for identification of ELS to lower taxonomic levels are fragile and frequently damaged during specimen collection and handling (e.g., cranial and opercular spines, developing fin elements). Therefore, meristics and cranial spination patterns are most useful for identification of postflexion and later life stages (Moser 1996). Hardy (2005) and Fahay (2007) provide meristic and other information for non-pteroine scorpaenids in the WNA.

Based on the ELS of the five pteroines discussed here and a review of the scorpaenid literature, one or more of the following characteristics distinguish larvae of *P. volitans* and the four members of *Dendrochirus* from non-pteroine scorpaenids and other morphologically similar taxa in the WNA: the presence or absence of a "shield" of pigment over the dorsolateral margin of the visceral mass (may be reduced or augmented with scattered blotches in larger larvae of some taxa); pectoral-fin length, shape, and pigmentation pattern; the presence or absence of a small slit behind the fourth gill arch; the length, placement, and appearance of the PPO spines; the presence or absence, and number of spines along the opercle; and the relative length, elevation, and placement of the parietal and nuchal spines (Table 5).

Early larvae of *Helicolenus dactylopterus* (Delaroche, 1809), and members of *Scorpaena* and *Sebastes* have a dusky to dark "shield" of pigment over the visceral mass (Moser 1996; Hardy 2005; Fahay 2007) that larvae of the five pteroines and other scorpaenids with ELS described lack. *Helicolenus dactylopterus* also has a mass of spongy tissue below the base of the spinous dorsal fin that easily distinguishes its larvae from other scorpaenid genera (Table 5). Members of *Pontinus*, *Scorpaenodes*, and *Ectreposebastes imus* Garman, 1899, lack a "shield" of pigment over the visceral mass and have a deeply embedded medial blotch of pigment just above the base of the pectoral fins that later expands to cover the dorsal surface of the gas bladder (Moser *et al*. 1977).

Differences in pectoral-fin length, shape, and pigmentation pattern can also help to distinguish some scorpaenids. *Pterois volitans* and the four members of *Dendrochirus* have elongate, lightly pigmented to mottled pectoral fins, whereas most non-pteroines have pigment (often pronounced) on some portion to most of the fin (Moser 1996). *Setarches guentheri* and *E. imus* also have elongate pectoral fins. Whereas small *E. imus* have most of the fin peppered with melanophores, except an unpigmented area near the inner margin that expands distally as larvae develop (Moser *et al*. 1977), the extent and location of pectoral fin pigment is unknown for *S. guentheri*. Members of *Scorpaena* and *Scorpaenodes* have rounded or fan-shaped pectoral fins of short to moderate length that seldom extend beyond the origin of the anal-fin base in *Scorpaena*, and may extend to or slightly beyond mid-anal-fin base in *Scorpaenodes* (Moser *et al*. 1977; Hardy 2005; Baldwin 2013). Larvae of members of *Scorpaena* also typically have some portion of the inner half to most of the pectoral fin heavily pigmented, with little to no pigment along its distal margin (Moser 1996; Hardy 2005; Baldwin 2013), whereas members of *Scorpaenodes* have nearly the entire pectoral fin heavily pigmented, which can make these fins appear larger than in other genera (Baldwin 2013). By comparison, larvae of *H. dactylopterus*, and those of members of *Sebaste*s in the WNA, have relatively short, fan-shaped pectoral fins with little to no pigment (Fahay 2007), and members of *Pontinus* have wing-shaped pectoral

fins (i.e., upper rays longer than lower) that extend to about mid-anal-fin base; fin pigmentation, however, is complex in *Pontinus* and develops through sequential stages (Sánchez & Acha 1988; Moser 1996; Fahay 2007). Although pectoral-fin ray counts overlap and are of little value for taxonomic discrimination in most scorpaenids (Moser *et al*. 1977), *S. guentheri* has more rays (≥22 in WNA; Eschmeyer & Collette 1966) than pteroine (Table 4) and other non-pteroine scorpaenids, except *T. cristulata*, with 22–24 rays (Eschmeyer 1969). Illustrations in Ginsburg (1953) provide additional insight into differences in shape of the pectoral fins for four scorpaenid taxa.

The presence or absence, number, and placement of spines along the opercle can also distinguish some scorpaenids. As previously mentioned, larvae of *P. volitans* and the four *Dendrochirus* lack spines on the opercle, as do juveniles and adults of these taxa (e.g., Matsunuma & Motomura 2016a, 2018; Matsunuma *et al*. 2017), whereas members of *Ebosia* and *Parapterois* have a single, raised spine on either the upper or lower margin of the opercle (Matsunuma & Motomura 2015a, 2016b, 2022), and *Brachypterois* spp. have a spine on the upper margin, and may or may not have a spine on the lower margin (Matsunuma *et al*. 2013). Most non-pteroine scorpaenids, however, have two spines on the opercle, except *H. dactylopterus* and members of *Sebastes*, which may have a small to tiny spine near the upper margin only (Fahay 2007).

Some scorpaenids also differ in the relative length, size, and placement of the parietal and nuchal spines (Table 5). *Pterois volitans*, *E. imus*, and members of *Scorpaena* and *Pontinus* have parietal spines two or more times longer than the nuchals, whereas the four members of *Dendrochirus* have parietal and nuchal spines subequal in length. Larvae of *H. dactylopterus* and most members of *Sebastes* have long parietal spines, and small to tiny nuchals that often form relatively late in development, while other members of *Sebastes* may lack nuchal spines entirely (Moser 1996; Fahay 2007). Members of *Scorpaenodes*, however, have an enlarged, crest-like parietal ridge that terminates in posteriorly placed nuchal spines similar in length or longer than the anteriorly positioned parietals (Moser 1996; Baldwin 2013; Kojima 2014).

Most scorpaenids in the WNA have a basic complement of five PPO spines as juveniles and adults (Ginsburg 1953), but patterns can be variable and complex, and counts can change during ontogeny in some taxa (Eschmeyer 1969; Moser 1996; Hardy 2005; Fahay 2007). The presence or absence, placement, and relative length of one or more of the PPO spines, however, can have taxonomic value for some taxa (Eschmeyer 1965, 1969; Eschmeyer & Collette 1966; Moser 1996). *Pterois volitans* has four relatively slender spines with the middle pair moderate in length and longer than the uppermost and lowermost, whereas the four members of *Dendrochirus* have five spines about evenly spaced along the shelf with the upper 3–4 spines subequal and longer than the lowermost. WNA members of *Sebastes* and larvae of *H. dactylopterus* also have spines of short to moderate length. In *Sebastes*, PPO-2 and -3 or PPO-2 through -4 are subequal and can be longer than the uppermost or lowermost, whereas *H. dactylopterus* has 3–4 relatively stout spines with the longest near the shelf angle (Fahay 2007). ELS of members of *Scorpaena* can have one or more robust spines with the longest typically near the shelf angle, whereas in later life stages and juveniles, PPO-1 or -2 may be the longest, and others can be reduced or absent (Ginsburg 1953; Eschmeyer 1969; Hardy 2005). Larvae of *Scorpaenodes* spp. can have two to four robust PPO spines (Moser 1996; Kojima 2014), but the crest-like parietal ridge, and typically longer nuchal than parietal spines, easily distinguishes these from most other WNA scorpaenids (Table 5). Early larvae of *S. guentheri*, *E. imus*, and *Pontinus* spp. have three robust PPO spines about evenly spaced along the shelf margin (Sánchez & Acha 1988; Moser 1996; Fahay 2007; Mertzlufft 2021), and larger larvae or pelagic juveniles of these taxa often add one or two additional spines. Members of *Pontinus* may also have the spine at the angle simple or serrate, and some species have supplemental PPO spines and one or more enlarged APO spines (Moser 1996). PPO-spine patterns illustrated in Ginsburg (1953) offer additional insight into differences in spine length and placement in other non-pteroine scorpaenids.

The number of spines along the ocular ridge and in the dorsal fin should be used cautiously as taxonomic characters, especially for small larvae. ELS of most scorpaenids have one to three spines along the ocular ridge, and some can be pronounced and project outward over the eye. Although early larvae of *Pontinus* spp. and *E. imus* have an enlarged, stout, forward-angled supraocular spine (Moser 1996; Fahay 2007; Mertzlufft 2021) that *P. volitans,* the four *Dendrochirus*, and most other non-pteroine scorpaenids lack, the ocular spines are often broken during specimen collection and handling, and may be resorbed in later life stages. Therefore, differences in the relative size and orientation of these spines have limited utility for identification purposes unless intact. Dorsal-spine counts also overlap in most WNA scorpaenids (Fahay 2007), and the spine at the origin of the soft dorsal fin may appear first as a ray and not ossify until much later (Eschmeyer & Collette 1966; Moser *et al*. 1977). Because the transition from ray to spine can also be gradual (Moser 1996), we suggest that total element counts for a given fin are a more useful taxonomic character for ELS.

TABLE 5. Discrimination of early life stages of *Pterois volitans*, *Dendrochirus barberi*, *D. hemprichi*, *D.* "*bellus*," and *D. zebra* from non-pteroine scorpaenids in the Western North Atlantic. Scorpaenids typically have five spines along the posterior shelf of the preopercle (PPO), although early larvae of some taxa may have three, and add one or two spines in subsequent life stages. "Elongate" spine(s) refer to those about two or more times longer than the next longest spine, or all spines that extend well beyond the posterior margin of the operculum or ventral margin of body, depending on orientation. "Robust" spines refer to "elongate" spines, as defined above, that are structurally stout and broad-based, whereas spines of short to moderate length are typically "slender" with a relatively narrow base. "Elongate" fins refer to those whose tips extend to, and typically well beyond, the posterior margin of the anal-fin base, whereas "short" fins may extend to, but seldom beyond, the origin of the anal-fin base. The pectoral fins are precocious, unless otherwise noted. "Shield" of pigment refers to the extent of pigmentation over the dorsolateral surface of the visceral mass in early larvae, which may be reduced or augmented with scattered blotches of pigment in larger larvae of some taxa. The parietal spines are typically two or more times longer than the nuchals, unless otherwise noted. Classification of subfamilies within Scorpaenidae follows van der Laan *et al*. (2023). Abbreviations: parietal spines (P), nuchal spines (N), anal-fin origin (AFO), anal-fin base (AFB). Characters compiled from Sánchez & Acha (1988); Moser (1996); Hardy (2005); Fahay (2007); Baldwin (2013); Kojima (2014); Mertzlufft (2021); and include the personal observations of the senior author.

Taxon	Relative size & length		Opercle spine(s)	Visceral mass	Pectoral fins		Slit behind 4th gill arch	Other characteristics
	(P)arietal & (N)uchal spines	PPO spines		"Shield" of pigment	Contour & length	Pigmentation		
Pteroinae								
Pterois volitans	P > N	Middle pair longer than outer; none distinctly elongate	None	No	Elongate, fan-shaped; tips to or beyond terminal margin of AFB	Light to mottled	No	Pigmentation sparse, typically concentrated along body midlines (until late transformation). Elevation of parietal & nuchal spines ~30° above longitudinal axis of head.
Dendrochirus spp.	N ≥ P	Upper 3–4 subequal, none distinctly elongate; all about evenly spaced	None	No	Elongate, fan-shaped; tips to or beyond terminal margin of AFB	Light to mottled	No	Pigmentation sparse until transformation, then saddles along dorsal & ventral margins. Elevation of parietal & nuchal spines low on head (≤15°).

.....*Continued on the next page*

TABLE 5. (Continued)

Taxon	Relative size & length		Opercle spine(s)	Visceral mass	Pectoral fins		Slit behind 4th gill arch	Other characteristics
	(P)arietal & (N)uchal spines	PPO spines		"Shield" of pigment	Contour & length	Pigmentation		
Scorpaeninae								
Pontinus spp.	P > N	One or more elongate & robust, spine near shelf angle typically longest	Pair near upper margin only	No [1]	Wing-shaped (upper rays longer than lower); tips to about mid-AFB	Variable, develops through sequential stages	Yes	Initially, three robust PPO's about evenly spaced along shelf. Some species may have one or more enlarged APO & supplemental PPO spines. Supraocular spine stout, may be forward-angled (if unbroken). Parietals enlarged, stout, nuchals minute (develop late). Pigment on spinous dorsal-fin becomes streak or blotch. Liver area may be dark or dusky.
Scorpaena spp.	P > N	Variable	Upper & lower margins	Yes	Fan-shaped; tips to AFO seldom beyond	Some to most of fin dark	No	Tips of pelvic fins short of anus. Inner half to most of pectoral fins well pigmented, distal margin may be unpigmented or sparsely so.
Scorpaenodes spp.	N ≥ P	2–4 stout, moderately elongate spines	Pair near upper margin only	No [1]	Fan-shaped; tips to about mid-AFB	Some to most of fin dark	Present or absent	Parietal ridge crest-like, nuchal & parietal spines pronounced. Heavy pigmentation makes pectoral fins appear superficially larger than in other genera.
Sebastinae								
Helicolenus dactylopterus	P > N	3–5 relatively stout, middle longest; none distinctly elongate	Single, small to tiny near upper margin only, if present	Yes	Fan-shaped; tips to or slightly beyond AFO	Sparse to none	Yes	Characteristic mass of spongy tissue below spinous dorsal-fin base. Caudal fin precedes pectoral fin development.

.....Continued on the next page

TABLE 5. (Continued)

Taxon	Relative size & length		Opercle spine(s)	Visceral mass	Pectoral fins		Slit behind 4th gill arch	Other characteristics
	(P)arietal & (N)uchal spines	PPO spines		"Shield" of pigment	Contour & length	Pigmentation		
Sebastes spp. [2]	P > N	Variable, spine at angle often longest; none distinctly elongate	Single, small to tiny near upper margin only, if present	Yes	Fan-shaped; tips to or slightly beyond AFO	Sparse to none	No	Prominent cluster of pigments on dorsal surface of head; postanal series of melanophores along dorsal & ventral midlines of body. Caudal fin development precedes that of pectoral fin. High count of 29–32 myomeres.
Setarchinae								
Ectreposebastes imus	P > N	Initially, three robust, about evenly spaced, longest near angle; one or two added in later life stages	Upper & lower margins	No [1]	Elongate, fan-shaped; tips to or beyond terminal margin of AFB	Most of fin, but becomes more distal at larger sizes	Yes	Supraocular spine may be stout, forward-angled (if unbroken). Parietals about three times longer than nuchals. Tip of lower jaw juts out slightly beyond upper jaw. Cranium cavernous, weakly ossified, transparent.
Setarches guentheri [3]	P > N	Upper 3–4 subequal, all about evenly spaced; none distinctly elongate	Upper & lower margins	Unknown	Elongate, fan-shaped; tips likely to or beyond terminal margin of AFB	Unknown	Yes	High modal count of 22–24 pectoral-fin rays. Cranium cavernous, weakly ossified, transparent. Pigment scattered over upper & lower surfaces of visceral mass likely.

[1] Deeply embedded medial blotch just above pectoral-fin base expands to cover dorsal surface of gas bladder (Moser *et al*. 1977)
[2] Nuchals, if present, small to tiny & form late, often posterior to base of parietals
[3] Some characters based on limited description in Mertzlufft (2021)

The presence or absence of a small slit behind the fourth gill arch (Table 5), differences in the number of total myomeres and fin elements, the order of fin development, the size and developmental state when released by the female, and the presence or absence of supplemental PPO spines can also be used to distinguish some taxa. The pectoral fins differentiate first in most pteroine and non-pteroine scorpaenids, except *Sebastes* spp. and *H. dactylopterus*, in which the primary caudal rays appear first (Kendall 1991; Nagasawa & Kojima 2014). WNA members of *Sebastes* also have more myomeres (29–32), and total dorsal-fin (≥26) and anal-fin elements (≥9, typically 10–12) than pteroine (Table 4) and other non-pteroine scorpaenids (e.g., 24–26 myomeres, ≤24 total dorsal-fin, and typically 8–9 total anal-fin elements). Larvae of *Sebastes* spp. also have a prominent "cephalid" cluster of pigment and a postanal series of melanophores along the dorsal and ventral midlines of the body that extend further anteriad than in other scorpaenid genera (Fahay 2007). The number of enlarged spines that project laterally along the IO ridge (Ginsburg 1953), and the presence or absence, and number of barbels on the snout, can also be used to distinguish some taxa, although these characters may not develop before the juvenile stage.

Based on personal observations and the characteristics of ELS of other sebastolobines from the Eastern Pacific (Moser 1996), small *T. cristulata* should be expected to have the following traits: a prominent, crest-like, parietal ridge with the nuchal spine longer than the parietal; a dusky "shield" or blotches of pigment over the dorsolateral surface of the visceral mass; and a series of stout PPO spines with the longest (i.e., PPO-1) aligned with the IO ridge. Postflexion or transforming larvae may also have pigment scattered over the pectoral-fin base and inner half of the rays, as in other sebastolobines (Moser 1996). In addition, small *T. cristulata* should have an elevated IO ridge with a series of 7–8 conspicuous, laterally projecting spines, and a dusky peritoneum; and lack a small slit behind the fourth gill arch, as noted for juveniles (Ginsburg 1953; Eschmeyer 1969). A high pectoral-fin count of 22–24 (mode 23) rays (Eschmeyer 1969) should also distinguish *T. cristulata* from other WNA scorpaenids, except *S. guentheri* (≥22 rays; Eschmeyer & Collette 1966).

Eschmeyer (1969) does not mention the ocular papillae that we observed in the juvenile *T. cristulata*. Ginsburg (1953), however, noted "short, slender filaments sparsely developed on upper part of eyeball," a character that has been described for other members of the genus (Motomura *et al.* 2007). Mertzlufft (2021) provides several low-resolution images of a larva designated "morphotype G," which we estimate to be about 8.5 mm SL based on image scale. Larvae of "morphotype G" lack a small slit behind the fourth gill arch, and have an elevated parietal ridge with a longer nuchal than parietal spine, characters possessed by some *Scorpaenodes* spp. in the WNA and members of Sebastolobinae to which *T. cristulata* belongs (Tables 5 & 6). Mertzlufft (2021) provided few other details, but *Scorpaenodes* spp. do not occur in the northern Gulf of Mexico (Hardy 2005) where the larvae he examined were collected. Because all other native scorpaenid genera in the WNA also have a longer parietal than nuchal spine (Table 6), we believe "morphotype G" to be larvae of *T. cristulata*.

Late postflexion and transforming larvae of *P. nebris* should be expected to have some combination of the following traits (Table 6): a series of 5–6 stout, laterally projecting spines along the IO ridge; a small slit behind the fourth gill arch; parietal and nuchal spines conjoined at the base with longer parietals than nuchals; and PPO-2 may be absent, or blunt and "knob-like." Their ELS may also have scattered blotches of pigment over the visceral mass; melanophores scattered over the pectoral-fin base and inner half of the rays, with the longest rays near mid-fin; and pelvic fins short of the anal-fin base. Once developed, a short, incomplete lateral line with 3–4 tubed scales immediately behind the head easily distinguishes *P. nebris* from all other WNA scorpaenids (Eschmeyer 1965). The short ocular papillae that we observed in *P. nebris* were not mentioned by Eschmeyer (1965, 1969) and have not been described for other members of the genus (Motomura *et al.* 2012) to our knowledge. Although these papillae are not an artifact of the preservation process, they may have been lost or resorbed at the larger sizes (i.e., late juveniles and adults) typically described by other authors.

Larvae of *Neomerinthe* spp. were not available for examination. Motomura *et al*. (2011), however, described an 18.4 mm *Neomerinthe naevosa* Motomura, Béarez & Causse, 2011 from the south-central Pacific as having a large head and deep body (i.e., HL 53.8% SL; body depth about 42% SL); parietal spines well developed and subequal to OD; minute nuchal spines; a dark blotch above the first and second pored lateral-line scales; a short, narrow band of pigment adjacent to the first dorsal spine; and a dark blotch between dorsal spines 7 and 11. Juvenile *Neomerinthe* spp. from the WNA have relatively short pelvic fins with the tips of the longest rays well short of the anal-fin base; PPO-1 typically has a supplemental spine at its base, and is longer than other PPO spines; and the gap between PPO-1 and -2 is wider than between those below (Eschmeyer 1969). In addition, the opercle has a pair of spines; 3–4 enlarged spines project laterally from the IO ridge; and the lateral line extends onto the base of the caudal fin (Eschmeyer 1969; Poss & Eschmeyer 2002; Motomura *et al*. 2011).

TABLE 6. Recognition and identification of the early life stages (ELS) of some poorly known deep-water members of Scorpaenidae from the Western North Atlantic. ELS are expected to share some characteristics of other members of the subfamily. Characters identified are based on the descriptions of larvae or juveniles in Eschmeyer (1965, 1969), Eschmeyer & Randall (1975), Moser *et al.* (1977), Moser (1996), Hardy (2005), Motomura *et al.* (2011), and Mertzlufft (2021), and augmented by the personal observations of the senior author for *Phenacoscorpius nebris* and *Trachyscorpia cristulata*. Classification of subfamilies within Scorpaenidae follows van der Laan *et al.* (2023). Abbreviations: parietal spines (P), nuchal spines (N), posterior shelf of the preopercle (PPO), anal-fin origin (AFO), anal-fin base (AFB), infraorbital ridge (IO). "Shield" of pigment refers to the extent of pigmentation over the dorsolateral surface of the visceral mass in early larvae, which may be reduced or augmented with scattered blotches in larger larvae of some taxa. The parietal spines are typically two or more times longer than the nuchals, unless otherwise noted.

Taxon	Relative size & length of spines		Opercle spine(s)	"Shield" of pigment over gut	Pectoral fins		Slit behind 4th gill arch	Other characteristics
	(P)arietal & (N)uchal	PPO			Contour & length	Pigmentation		
Scorpaeninae								
Idiastion kyphos	P > N likely	Unknown	Upper & lower margins	Unknown	Longest rays near upper part of fin; tips not beyond anal spines	Unknown	Yes	Pronounced gap between PPO-1 and -2. Membrane between dorsal spines low, about 50% of each spine exposed. Tips of lower 10 pectoral-fin rays free from membrane; tips of pelvic-fin rays short of AFO.
Neomerinthe spp. [1]	P > N	PPO-1 longest; gap between PPO-1 and -2 wider than those below	Upper & lower margins	Unlikely	Fan-shaped; tips not beyond mid-AFB	Unknown	Yes [2]	Stout parietal ridge, small nuchals. IO ridge with series of 3–4 stout, laterally projecting spines. Tips of pelvic-fin rays short of AFO.
Phenacoscorpius nebris	P > N	Typically, PPO-1 adjacent to IO ridge longest; PPO-2 "knob-like" or absent	Upper & lower margins	Scattered blotches likely	Middle rays longest; tips of longest rays perhaps to mid-AFB, others to about AFO	Fin base & inner half of rays, or some part thereof	Yes	Series of 5–6 stout, laterally projecting spines along IO ridge. Tips of pelvic-fin rays short of AFO. Pigment between fifth & ninth dorsal spines; fin base & inner half of dorsal & anal fins dusky. Very short lateral line.
Sebastolobinae								
Trachyscorpia cristulata	N > P	PPO-1 about two times longer than PPO-2, those below progressively shorter	Upper & lower margins	Dusky shield, or scattered blotches likely	Upper rays longest; tips to or slightly beyond AFO	Fin base & inner half of rays, or some part thereof	No	Parietal ridge elevated, terminates in longer nuchal than parietal spine. Series of 7–8 stout, laterally projecting spines along IO ridge. High modal pectoral-fin count of 22–23 rays. Peritoneum dusky. Lateral line complete.

[1] Most head spines and other structures in 18.4 mm juvenile from south-central Pacific same as those of adults per Motomura *et al.* (2011)

[2] Applies to Atlantic species only because some Pacific species lack said character per Motomura *et al.* (2011)

Searobin larvae (Family Triglidae) can resemble those of the lionfishes. In fact, larvae of *Prionotus ophryas* Jordan & Swain, 1885 were originally identified as *P. volitans* (Victor & Ianniello 2020). Triglids, however, have a combination of characters not found in other scorpaeniform fishes: a large bony head; duck-like, concave snout profile; and pectoral fins peppered with small melanophores that extend to about the middle of the anal-fin base, with ≤14 (often 12–13) rays, plus 2–3 free, finger-like lower rays (Richards 2005a). Triglid larvae also typically have small melanophores scattered over the snout and operculum; have a series of postanal melanophores along the ventral midline; have relatively short, low parietal and nuchal spines; lack or have short PPO spines; and have ≤11 dorsal spines with a deep notch between the spinous and soft-dorsal fins, whereas WNA members of Scorpaenidae have ≥12 dorsal spines (Richards 2005a; Fahay 2007). Triglids also lack spines in the anal fin, and may have spines along the interopercle or subopercle (Richards 2005a).

Other regional scorpaeniforms include dactylopterids (flying gurnards) and peristediids (armored searobins). Dactylopterids have large eyes; a heavily armored head with robust, extremely pronounced supraocular and PPO spines; a low myomere count of 22; a total of 14 dorsal-fin and 6 anal-fin elements; and ≥30 pectoral-fin rays. Dactylopterids also have a greatly enlarged nuchal spine with a small parietal spine at its base, and postflexion larvae have hook-like spinules along the posteroventral margin of the longest PPO spine (Fahay 2007). By comparison, peristediid larvae have: a slender, elongate body; 13–15 pectoral-fin rays (one species with 16 rays) that seldom extend beyond mid-anal-fin base, with several upper rays filamentous and longer than those below (if unbroken); 33–35 myomeres and ≥15 anal-fin rays (often 17–20); highly elevated supraocular and nuchal spines; a pronounced nasal spine and/or spine on IO1; and other ornate head spines (Richards 2005b).

Larvae of some members of the former serranid subfamily Anthiadinae (now Anthiadidae) superficially resemble those of the lionfishes, but anthiads have a large, sometimes rugose head, and an enlarged PPO spine that overlays a spine on the interopercle, which gives the operculum a double spine appearance. Anthiads also have: a deep, kite-shaped body; precocious dorsal and pelvic spines, with the second or third dorsal spine notably longer than the others; pigment in blotches on the body and/or median fins; and some species have a cockscomb-like supraoccipital crest (Richards *et al.* 2005; Fahay 2007). Anthiads also lack parietal and nuchal spines.

Lionfishes in marine ornamental trade

The risks associated with introduction of other species of lionfishes in the marine ornamental trade appears low, but vary across the subfamily (Lyons *et al.* 2020). The trade imports *P. volitans* and *D. zebra* at moderate to high volumes, and *D. biocellatus* (Fowler, 1938) and individuals "identified" as *D. brachypterus* and *P. radiata* at moderate to low volumes (Lyons *et al.* 2020). Other members of *Pterois* and *Dendrochirus* occur infrequently, ship poorly, or are difficult to keep in captivity (Marini 2010; Fenner 2012), and some are rare in nature (e.g., *P. andover*) or known only from the holotype (e.g., *D. tuamotuensis* Matsunuma & Motomura, 2013a; *D. koyo* Matsunuma & Motomura, 2019). Members of *Parapterois* are rare, and those of *Brachypterois* and *Ebosia* are unknown in trade (Marini 2010; Fenner 2012).

Most lionfishes imported into the U.S. originate from Kenya, Sri Lanka, Indonesia, or the Philippines (Lyons *et al.* 2019). Taxonomic ambiguity due to the morphological similarity of some taxa, and the use of multiple common names for the same species, or same common name for different species makes the lionfishes difficult to track in trade. Because hobbyists remain the likely pathway of introduction for invasive species (Lyons *et al.* 2019), ambiguity in nomenclature elevates the risk of misidentification. For example, lionfishes collected throughout the Indo-Pacific and sold as "*P. volitans*" may be a complex of *P. miles* and *P. russelii* (Wilcox *et al.* 2018; Lyons *et al.* 2019); lionfishes collected off Kenya and along the Red Sea identified as *D. brachypterus* refer to *D. hemprichi* (Matsunuma *et al.* 2017); and lionfishes identified as *P. radiata* from the Red Sea area refer to *P. cincta* (Matsunuma & Motomura 2016a). Misidentifications also create uncertainty in our knowledge of reproductive biology and behavior, temperature tolerance limits, and understanding invasive potential. In fact, information on reproductive biology in Fishelson (1975, 1978, 1997), and ELS molecularly identified as *D. brachypterus* from the Red Sea in Kimmerling *et al*. (2018) refer to *D. hemprichi* (Matsunuma *et al.* 2017). Egg morphology and reproductive behavior described in Fishelson (1975) and individuals molecularly identified as *P. radiata* from the Red Sea in Kimmerling *et al*. (2018) refer to *P. cincta* (Matsunuma & Motomura 2016a). Behaviors attributed to *P. volitans* from the Red Sea area in Fishelson (1997) refer to *P. miles* or *P. cincta* (Matsunuma & Motomura 2016a).

We support the recommendation of Lyons *et al*. (2019) that future research apply proactive risk assessment screening to identify species of invasive concern to better inform management decisions. For the lionfishes, however, screening candidates for invasive potential will remain problematic until identification guides are developed to distinguish currently valid species, and this information can be disseminated to marine vendors, hobbyists, researchers, and decision-makers. Development of such a guide would encourage vendors to identify and segregate imports, which would enhance our ability to track lionfishes in the marine ornamental trade.

Acknowledgments

This manuscript includes specimens collected by NOAA during the Deepwater Horizon Natural Resource Damage Assessment and work conducted cooperatively with academic institutions, other federal and state trustees, and British Petroleum. It also includes supplemental material collected during NOAA ichthyoplankton surveys of the Western Caribbean. Thanks to Rick Feeney (deceased), formerly of LACM for the loan of larval *D. barberi* and the juvenile *D. hemprichi* from museum collections; to Tracey Sutton, Nova Southeastern University, Fort Lauderdale, Florida, and to Glenn Zapfe, NOAA, Southeast Fisheries Science Center, Pascagoula, Mississippi for the loan of *P. volitans* larvae housed at those institutions; and to Jay Rooker, Texas A&M University, Galveston, who provided the two flexion larvae of *P. volitans*. A special thanks to Junichi Kojima, fellow of the Marine Ecology Research Institute, Tokyo, and Tokai University Press, Hadano, for permission to use the illustrations of *D. zebra* and *D.* "*bellus*," and to Mohamed Abu El-Regal, King Abdullah University of Science and Technology, Jeddah, Saudi Arabia for permission to use his images of a *D. hemprichi* larva collected in the Red Sea. Thanks to Claudia Traboni of the Instituto de Ciencias del Mar-Consejo Superior de Investigaciones Científicas (ICM-CSIC, Spain) for efforts to digitally enhance images of *P. volitans*, *D. barberi*, and *D. hemprichi*. Thanks to Amanda Dauman of Amanda Levine Art, Town of East Hampton, New York, and to Eric Fortman, Florida Fish Wildlife Research Institute, both formerly of the University of Miami's Cooperative Institute for Marine and Atmospheric Science (CIMAS) for support in making preliminary illustrations of *P. volitans* larvae. Thanks to Sandra Raredon (retired), formerly of the Smithsonian Institution's National Museum of Natural History (NMNH), Museum Support Center, for the image of the juvenile *D. hemprichi* and radiograph of the aberrant *P. volitans*, and to Alan Collins and Tom Munroe of NOAA's National Systematics Lab at NMNH, as well as G. David Johnson of NMNH for space and access to literature and other resources while the senior author was a visiting scientist. We also gratefully acknowledge the assistance of Cheryl Ames, Smithsonian Associate, who translated Kojima's work from Japanese to English. Thanks to NOAA's Southeast Fisheries Science Center (SEFSC), Galveston, who provided institutional support for the senior author during manuscript preparation. CIMAS at the University of Miami, Florida (Cooperative Agreement #NA15OAR43200064) provided institutional support for E. Malca, and El Colegio de la Frontera Sur, Unidad Chetumal, Quintana Roo, Mexico provided institutional support for L. Vásquez-Yeomans. Thanks also to the staff at ECOSUR (Chetumal, Mexico) and the SEFSC, Miami Lab, for support with *P. volitans* imaging and processing during the initial years of the Atlantic invasion. The senior author dedicates this paper to his eldest son, Ryan, who lost his bout with pancreatic cancer in 2021.

References

Adcroft, A., Hallberg, R., Dunne, J.P., Samuels, B.L., Galt, J.A., Barker, C.H. & Payton, D. (2010) Simulations of underwater plumes of dissolved oil in the Gulf of Mexico. *Geophysical Research Letters*, 37 (18), L18605. https://doi.org/10.1029/2010GL044689

Ahlstrom, E.H., Butler, J.L. & Sumida, B.Y. (1976) Pelagic stromateoid fishes (Pisces, Perciformes) of the eastern Pacific: kinds, distributions, and early life histories and observations on five of these from the Northwest Atlantic. *Bulletin of Marine Science*, 26 (3), 285–402.

Ahrenholz, D.W. & Morris, J.A., Jr. (2010) Larval duration of the lionfish, *Pterois volitans* along the Bahamian Archipelago. *Environmental Biology of Fishes*, 88 (4), 305–309. https://doi.org/10.1007/s10641-010-9647-4

Albins, M.A. (2015) Invasive Pacific lionfish *Pterois volitans* reduce abundance and species richness of native Bahamian coral-reef fishes. *Marine Ecology Progress Series*, 522, 231–243. https://doi.org/10.3354/meps11159

Allen, G.R. & Erdmann, M.V. (2008) *Pterois andover*, a new species of scorpionfish (Pisces: Scorpaenidae) from Indonesia and Papua New Guinea. *Aqua*, *International Journal of Ichthyology*, 13 (3–4), 127–138.
Baldwin, C.C. (2013) The phylogenetic significance of colour patterns in marine teleost larvae. *Zoological Journal of the Linnean Society*, 168 (3), 496–563. https://doi.org/10.1111/zoj.12033
Bariche, M., Kleitou, P., Kalogirou, S. & Bernardi, G. (2017) Genetics reveal the identity and origin of the lionfish invasion in the Mediterranean Sea. *Scientific Reports*, 7, 6782. https://doi.org/10.1038/s41598-017-07326-1
Baur, H. & Leuenberger, C. (2011) Analysis of ratios in multivariate morphometry. *Systematic Biology* 60 (6), 813–825. https://doi.org/10.1093/sysbio/syr061
Bennett, E.T. (1831) Characters of a new species of *Pterois*. *Proceedings of the Committee of Science and Correspondence of the Zoological Society of London*, 1830–1831, Part 1, 128. [https://www.biodiversitylibrary.org/item/46215#page/142/mode/1up]
Bennett, J.W. (1828) *A Selection from the Most Remarkable and Interesting Fishes Found on the Coast of Ceylon*. Edward Bull, London, 30 pp.
Bloch, M.E. (1787) *Naturgeschichte der ausländischen Fische*. *Dritter Theil*. M.E. Bloch, Berlin, 146 pp. https://doi.org/10.5962/bhl.title.63303
Byron, D., Heck, K.L., Jr. & Kennedy, M.A. (2014) Presence of juvenile lionfish in a Northern Gulf of Mexico nursery habitat. *Gulf of Mexico Science*, 32 (1–2), 75–77. https://doi.org/10.18785/goms.3201.08
Clarke, T.A. (1991) Larvae of nearshore fishes in oceanic waters near Oahu, Hawaii. *NOAA Technical Report NMFS*, 101, 1–19.
Cohen, F.P.A., Valenti, W.C. & Calado, R. (2013) Traceability issues in the trade of marine ornamental species. *Reviews in Fisheries Science*, 21 (2), 98–111. https://doi.org/10.1080/10641262.2012.760522
Côté, I.M. & Green, S.J. (2012) Potential effects of climate change on a marine invasion: the importance of current context. *Current Zoology*, 58 (1), 1–8. https://doi.org/10.1093/czoolo/58.1.1
Côté, I.M., Green, S.J. & Hixon, M.A. (2013) Predatory fish invaders: insights from Indo-Pacific lionfish in the western Atlantic and Caribbean. *Biological Conservation*, 164, 50–61. https://doi.org/10.1016/j.biocon.2013.04.014
Crooks, J.A. (2005) Lag times and exotic species: the ecology and management of biological invasions in slow-motion. *Écoscience*, 12 (3), 316–329. https://doi.org/10.2980/i1195-6860-12-3-316.1
Cuvier, G. & Valenciennes, A. (1829) *Histoire naturelle des poissons*. *Tome quatrième.* F.G. Levrault, Paris, 518 pp. https://doi.org/10.5962/bhl.title.7339
Dahl, K.A., Patterson, W.F., III, Robertson, A. & Ortmann, A.C. (2017) DNA barcoding significantly improves resolution of invasive lionfish diet in the Northern Gulf of Mexico. *Biological Invasions*, 19 (6), 1917–1933. https://doi.org/10.1007/s10530-017-1407-3
Delaroche, F.E. (1809) Suite du mémoire sur les espèces de poissons observées à Iviça. *Annales du Muséum d'Histoire Naturelle*, *Paris*, 13, 313–361, pls. 20–25.
Eschmeyer, W.N. (1965) Three new scorpionfishes of the genera *Pontinus*, *Phenacoscorpius* and *Idiastion* from the western Atlantic Ocean. *Bulletin of Marine Science*, 15 (3), 521–534.
Eschmeyer, W.N. (1969) A systematic review of the scorpionfishes of the Atlantic Ocean (Pisces: Scorpaenidae). *Occasional Papers of the California Academy of Sciences*, 79, 1–143.
Eschmeyer, W.N. & Collette, B.B. (1966) The scorpionfish subfamily Setarchinae, including the genus *Ectreposebastes*. *Bulletin of Marine Science*, 16 (2), 349–375.
Eschmeyer, W.N. & Rama-Rao, K.V. (1978) A new scorpionfish, *Ebosia falcata* (Scorpaenidae, Pteroinae), from the western Indian Ocean, with comments on the genus. *Matsya*, 3, 64–71.
Eschmeyer, W.N. & Randall, J.E. (1975) The scorpaenid fishes of the Hawaiian Islands, including new species and new records (Pisces: Scorpaenidae). *Proceedings of the California Academy of Sciences*, 40 (11), 265–333.
Evangelista, P.H., Young, N.E., Schofield, P.J. & Jarnevich, C.S. (2016) Modeling suitable habitat of invasive red lionfish *Pterois volitans* (Linnaeus, 1758) in North and South America's coastal waters. *Aquatic Invasions*, 11 (3), 313–326. https://doi.org/10.3391/ai.2016.11.3.09
Fahay, M.P. (2007) Scorpaeniformes, Part 1. *In*: Fahay, M.P. (Ed.), *Early Stages of Fishes in the Western North Atlantic Ocean* (*Davis Strait, Southern Greenland and Flemish Cap to Cape Hatteras*). *Vol. 2*. *Scorpaeniformes through Tetraodontiformes*. Northwest Atlantic Fisheries Organization, Halifax, Nova Scotia, pp. 932–981.
Fenner, B. (2012) The dwarf lions. *Tropical Fish Hobbyist*, 60 (April issue), 86–91.
Fishelson, L. (1975) Ethology and reproduction of pteroid fishes found in the Gulf of Aqaba (Red Sea), especially *Dendrochirus brachypterus* (Cuvier), (Pteroidae, Teleostei). *Pubblicazioni della Stazione Zoologica di Napoli*, 39 (Supplement 1), 635–656.

Fishelson, L. (1978) Oogenesis and spawn formation in the pigmy lion fish *Dendrochirus brachypterus* (Pteroidae). *Marine Biology*, 46 (4), 341–348.
https://doi.org/10.1007/BF00391406
Fishelson, L. (1997) Experiments and observations on food consumption, growth and starvation in *Dendrochirus brachypterus* and *Pterois volitans* (Pteroinae, Scorpaenidae). *Environmental Biology of Fishes*, 50 (4), 391–403.
https://doi.org/10.1023/A:1007331304122
Fogg, A.Q., Brown-Peterson, N.J. & Peterson, M.S. (2017) Reproductive life history characteristics of invasive red lionfish (*Pterois volitans*) in the northern Gulf of Mexico. *Bulletin of Marine Science*, 93 (3), 791–813.
https://doi.org/10.5343/bms.2016.1095
Fowler, H.W. (1938) Descriptions of new fishes obtained by the United States Bureau of Fisheries steamer "Albatross", chiefly in Philippine Seas and adjacent waters. *Proceedings of the United States National Museum*, 85 (3032), 31–135.
https://doi.org/10.5479/si.00963801.85-3032.31
Fricke, R., Eschmeyer, W.N. & van der Laan, R. (Eds.) (2023) Eschmeyer's Catalog of Fishes: Genera, Species, References. Available from: https://researcharchive.calacademy.org/research/ichthyology/catalog/fishcatmain.asp (accessed 1 July 2023)
Garman, S. (1899) Reports on an exploration off the west coasts of Mexico, Central and South America, and off the Galapagos Islands, in charge of Alexander Agassiz, by the U. S. Fish Commission steamer "Albatross," during 1891, Lieut. Commander Z. L. Tanner, U.S.N., Commanding. XXVI. The Fishes. *Memoirs of the Museum of Comparative Zoology*, 24, 3–431.
https://doi.org/10.5962/bhl.part.27494
Ginsburg, I. (1953) Western Atlantic scorpionfishes. *Smithsonian Miscellaneous Collections*, 121 (8), 1–103.
Goode, G.B. & Bean, T.H. (1896) XXXVI. Oceanic ichthyology, a treatise on the deep-sea and pelagic fishes of the world, based chiefly upon the collections made by the steamers Blake, Albatross, and Fish Hawk in the northwestern Atlantic, with an atlas containing 417 figures. *United States National Museum*, *Special Bulletin*, 2, i–xxxv + 1–26 + 1–553, Atlas, i–xxiii + 1–26, 123 pls.
https://doi.org/10.5962/bhl.title.48521
Grieve, B.D., Curchitser, E.N. & Rykaczewski, R.R. (2016) Range expansion of the invasive lionfish in the Northwest Atlantic with climate change. *Marine Ecology Progress Series*, 546, 225–237.
https://doi.org/10.3354/meps11638
Gunselman, S.R. & Spruell, P. (2019) Variation in life history may allow colonization of diverse habitats in an invasive fish species. *Copeia*, 107 (1), 124–130.
https://doi.org/10.1643/CI-18-072
Hamner, R.M., Freshwater, D.W. & Whitfield, P.E. (2007) Mitochondrial cytochrome *b* analysis reveals two invasive lionfish species with strong founder effects in the western Atlantic. *Journal of Fish Biology*, 71 (Supplement B), 214–222.
https://doi.org/10.1111/j.1095-8649.2007.01575.x
Hardy, J.D. (2005) Scorpaenidae: scorpionfishes. *In*: Richards, W.J. (Ed.), *Early Stages of Atlantic Fishes*: *An Identification Guide for the Western Central North Atlantic*. *Vol. 1*. CRC Press, Boca Raton, Florida, pp. 1141–1180.
https://doi.org/10.1201/9780203500217
Hunter, M.E, Beaver, C.E., Johnson, N.A., Bors, E.K., Mignucci-Giannoni, A.A., Silliman, B.R., Buddo, D., Searle, L. & Díaz-Ferguson, E. (2021) Genetic analysis of red lionfish *Pterois volitans* from Florida, USA, leads to alternative North Atlantic introduction scenarios. *Marine Ecology Progress Series*, 675, 133–151.
https://doi.org/10.3354/meps13841
Imamura, H. & Yabe, M. (1996) Larval record of a red firefish, *Pterois volitans*, from Northwestern Australia (Pisces: Scorpaeniformes). *Bulletin of the Faculty of Fisheries*, *Hokkaido University*, 47 (2–3), 41–46.
Incardona, J.P., Gardner, L.D., Linbo, T.L., Brown, T.L., Esbaugh, A.J., Mager, E.M., Stieglitz, J.D., French, B.L., Labenia, J.S., Laetz, C.A., Tagal, M., Sloan, C.A., Elizur, A., Benetti, D.D., Grosell, M., Block, B.A. & Scholz, N.L. (2014) *Deepwater Horizon* crude oil impacts the developing hearts of large predatory pelagic fish. *Proceedings of the National Academy of Sciences*, 111 (15), E1510–E1518.
https://doi.org/10.1073/pnas.1320950111
Johnson, J.Y. (1862) Descriptions of some new genera and species of fishes obtained at Madeira. *Proceedings of the Zoological Society of London*, 1862, 167–180.
Johnston, M.W. & Purkis, S.J. (2011) Spatial analysis of the invasion of lionfish in the western Atlantic and Caribbean. *Marine Pollution Bulletin*, 62 (6), 1218–1226.
https://doi.org/10.1016/j.marpolbul.2011.03.028
Johnston, M.W. & Purkis, S.J. (2014) Lionfish in the eastern Pacific: a cellular automaton approach to assessing invasion risk. *Biological Invasions*, 16 (12), 2681–2695.
https://doi.org/10.1007/s10530-014-0696-z
Jordan, D.S. & Hubbs, C.L. (1925) Record of fishes obtained by David Starr Jordan in Japan, 1922. *Memoirs of the Carnegie Museum*, 10 (2), 93–346.
https://doi.org/10.5962/p.234844
Jordan, D.S. & Swain, J. (1885) Description of three new species of fishes (*Prionotus stearnsi*, *Prionotus ophryas*, and *Anthias vivanus*) collected at Pensacola, Florida, by Mr. Silas Stearns. *Proceedings of the United States National Museum*, 7 (465),

541–545.
https://doi.org/10.5479/si.00963801.7-465.541
Jud, Z.R., Nichols, P.K. & Layman, C.A. (2015) Broad salinity tolerance in the invasive lionfish *Pterois* spp. may facilitate estuarine colonization. *Environmental Biology of Fishes*, 98 (1), 135–143.
https://doi.org/10.1007/s10641-014-0242-y
Kaluza, P., Kölzsch, A., Gastner, M.T. & Blasius, B. (2010) The complex network of global cargo ship movements. *Journal of The Royal Society Interface*, 7 (48), 1093–1103.
https://doi.org/10.1098/rsif.2009.0495
Kanayama, T. & Amaoka, K. (1981) First record of the scorpaenid fish *Brachypterois serrulatus* from Japan, with a key to Japanese genera of the Pteroinae. *Japanese Journal of Ichthyology*, 28 (2), 181–183.
https://doi.org/10.11369/jji1950.28.181
Kendall, A.W., Jr. (1991) Systematics and identification of larvae and juveniles of the genus *Sebastes*. *Environmental Biology of Fishes*, 30 (1–2), 173–190.
https://doi.org/10.1007/BF02296888
Kimmerling, N., Zuqert, O., Amitai, G., Gurevich, T., Armoza-Zvuloni, R., Kolesnikov, I., Berenshtein, I., Melamed, S., Gilad, S., Benjamin, S., Rivlin, A., Ohavia, M., Paris, C.B., Holzman, R., Kiflawi, M. & Sorek, R. (2018) Quantitative species-level ecology of reef fish larvae via metabarcoding. *Nature Ecology & Evolution*, 2, 306–316.
https://doi.org/10.1038/s41559-017-0413-2
Kitchens, L.L., Paris, C.B., Vaz, A.C., Ditty, J.G., Cornic, M., Cowan, J.H. Jr. & Rooker, J.R. (2017) Occurrence of invasive lionfish (*Pterois volitans*) larvae in the northern Gulf of Mexico: characterization of dispersal pathways and spawning areas. *Biological Invasions*, 19 (7), 1971–1979.
https://doi.org/10.1007/s10530-017-1417-1
Kletou, D., Hall-Spencer, J.M. & Kleitou, P. (2016) A lionfish (*Pterois miles*) invasion has begun in the Mediterranean Sea. *Marine Biodiversity Records*, 9, 46.
https://doi.org/10.1186/s41200-016-0065-y
Kojima, J. (2014) Scorpaenidae. *In*: Okiyama, M. (Ed.), *An Atlas of the Early Stages of Fishes in Japan*. *Second edition*. Tokai University Press, Hadano, pp. 607–628. [in Japanese]
Koya, Y. & Muñoz, M. (2007) Comparative study on ovarian structures in scorpaenids: possible evolutional process of reproductive mode. *Ichthyological Research*, 54 (3), 221–230.
https://doi.org/10.1007/s10228-006-0394-7
Lazarre, D. (2016) *Examining the Lionfish Invasion: How Growth and Recruitment Relates to Connectivity and Controls*. Ph.D. Dissertation, University of Miami, Coral Gables, Florida, xiv + 135 pp.
Leis, J.M. & Carson-Ewart, B.M. (Eds.) (2000) *The Larvae of Indo-Pacific Coastal Fishes*: *An Identification Guide to Marine Fish Larvae*. Fauna Malesiana Handbook 2, Brill, Leiden, 850 pp.
https://doi.org/10.1163/9789004474857
Levine, A. (2015) *Description and Illustrations of the Invasive Red Lionfish (Pterois volitans) from the Western Caribbean*. Master's Thesis, School of Marine and Atmospheric Sciences, Stony Brook University, New York, New York, 21 pp.
Linnaeus, C. (1758) *Systema naturae per regna tria naturae, secundum classes, ordines, genera, species, cum characteribus, differentiis, synonymis, locis*. *Editio decima*. *Vol*. *1*. Laurentii Salvii, Stockholm, 824 pp.
https://doi.org/10.5962/bhl.title.542
Lo-Yat, A. (1998) *Guide pratique pour la reconnaissance des larves et juveniles de quelques poissons lagonaires de Polynésie Française*. Annexe 6. Convention d'etude Service des Ressources Marines, Territoire de la Polynésie Française, 37 pp.
Lyons, T.J., Tuckett, Q.M., Durland Donahou, A. & Hill, J.E. (2020) Risk screen of lionfishes, *Pterois*, *Dendrochirus*, and *Parapterois*, for southeastern United States coastal waters of the Gulf of Mexico and Atlantic Ocean. *Biological Invasions*, 22 (5), 1573–1583.
https://doi.org/10.1007/s10530-020-02203-x
Lyons, T.J., Tuckett, Q.M. & Hill, J.E. (2019) Characterizing the US trade in lionfishes. *PLoS ONE*, 14 (8), e0221272.
https://doi.org/10.1371/journal.pone.0221272
Maamaatuaiahutapu, M., Remoissenet, G. & Galzin, R. (2006) *Guide d'identification des larves de poissons récifaux de Polynésie française*. Éditions Téthys, Taravao, Polynésie Française, 104 pp.
Mandrytsa, S.A. (2002) A new species of the genus *Pteropterus* (Scorpaenidae, Scorpaeniformes) from the Indian Ocean. *Journal of Ichthyology*, 42 (1), 124–125.
Marini, F.C. (2010) *Lionfishes and Other Scorpionfishes*. *The Complete Guide to the Successful Care and Breeding of These Spectacular and Popular Marine Fish*. *First Edition*. TFH Publications, Inc., Neptune, New Jersey, 128 pp.
Matsunuma, M. & Motomura, H. (2011) First records of a lionfish, *Pterois mombasae* (Scorpaenidae: Pteroinae), from Japan, and morphological comparisons with *P*. *antennata*. *Japanese Journal of Ichthyology*, 58 (1), 27–40.
https://doi.org/10.11369/jji.58.27
Matsunuma, M. & Motomura, H. (2013a) A new lionfish of the genus *Dendrochirus* (Scorpaenidae: Pteroinae) from the Tuamotu Archipelago, South Pacific Ocean. *Species Diversity*, 18 (1), 1–7.
https://doi.org/10.12782/sd.18.1.001
Matsunuma, M. & Motomura, H. (2013b) Newly recognized diagnostic characters of the poorly known lionfish *Pterois*

brevipectoralis (Scorpaenidae: Pteroinae), with notes on fresh coloration. *Species Diversity*, 18 (2), 163–173. https://doi.org/10.12782/sd.18.2.163
Matsunuma, M. & Motomura, H. (2015a) A new species of scorpionfish, *Ebosia saya* (Scorpaenidae: Pteroinae), from the western Indian Ocean and notes on fresh coloration of *Ebosia falcata*. *Ichthyological Research*, 62 (3), 293–312. https://doi.org/10.1007/s10228-014-0445-4
Matsunuma, M. & Motomura, H. (2015b) *Pterois paucispinula*, a new species of lionfish (Scorpaenidae: Pteroinae) from the western Pacific Ocean. *Ichthyological Research*, 62 (3), 327–346. https://doi.org/10.1007/s10228-014-0451-6
Matsunuma, M. & Motomura, H. (2016a) Redescriptions of *Pterois radiata* and *Pterois cincta* (Scorpaenidae: Pteroinae) with notes on geographic morphological variations in *P. radiata*. *Ichthyological Research*, 63 (1), 145–172. https://doi.org/10.1007/s10228-015-0483-6
Matsunuma, M. & Motomura, H. (2016b) A new species of scorpionfish, *Ebosia vespertina* (Scorpaenidae: Pteroinae), from the southwestern Indian Ocean. *Ichthyological Research*, 63 (1), 110–120. https://doi.org/10.1007/s10228-015-0479-2
Matsunuma, M. & Motomura, H. (2017) Indian Ocean record of *Brachypterois curvispina* Matsunuma, Sakurai & Motomura, 2013 (Scorpaenidae: Pteroinae) – a misidentification of *B. serrulifer* Fowler, 1938. *FishTaxa*, 2 (3), 123–125.
Matsunuma, M. & Motomura, H. (2018) Redescription and geographic variations of *Pterois antennata* and first record of *Pterois paucispinula* from French Polynesia (Scorpaenidae: Pteroinae). *Species Diversity*, 23 (1), 95–114. https://doi.org/10.12782/specdiv.23.95
Matsunuma, M. & Motomura, H. (2019) Redescription of *Dendrochirus zebra* (Scorpaenidae: Pteroinae) with a new species of *Dendrochirus* from the Ogasawara Islands, Japan. *Ichthyological Research*, 66 (3), 353–384. https://doi.org/10.1007/s10228-019-00681-1
Matsunuma, M. & Motomura, H. (2022) Revision of the genus *Parapterois* (Scorpaenidae: Pteroinae) and resurrection of *Parapterois nigripinnis* (Gilchrist 1904). *Ichthyological Research*, 69 (4), 401–432. https://doi.org/10.1007/s10228-021-00845-y
Matsunuma, M., Bogorodsky, S.V., Motomura, H. & Osman Mal, A. (2016) Objective record of *Pterois russelii* (Scorpaenidae: Pteroinae) from the Red Sea. *Cybium*, 40 (4), 333–337.
Matsunuma, M., Motomura, H. & Bogorodsky, S.V. (2017) Review of Indo-Pacific dwarf lionfishes (Scorpaenidae: Pteroinae) in the *Dendrochirus brachypterus* complex, with description of a new species from the western Indian Ocean. *Ichthyological Research*, 64 (4), 369–414. https://doi.org/10.1007/s10228-017-0583-6
Matsunuma, M., Padate, V.P. & Motomura, H. (2018) Re-assessment of a recent Indian Ocean record of the endemic East Asian species *Dendrochirus bellus* (Actinopterygii: Scorpaenidae: Pteroinae). *Acta Ichthyologica et Piscatoria*, 48 (1), 79–81. https://doi.org/10.3750/AIEP/02332
Matsunuma, M., Sakurai, M. & Motomura, H. (2013) Revision of the Indo-West Pacific genus *Brachypterois* (Scorpaenidae: Pteroinae), with description of a new species from northeastern Australia. *Zootaxa*, 3693 (4), 401–440. https://doi.org/10.11646/zootaxa.3693.4.1
McMenamin, S.K. & Parichy, D.M. (2013) Metamorphosis in teleosts. *In*: Shi, Y.-B. (Ed.), *Current Topics in Developmental Biology*. *Vol. 103*. Academic Press, San Diego, pp. 127–165. https://doi.org/10.1016/B978-0-12-385979-2.00005-8
McNutt, M.K., Camilli, R., Crone, T.J., Guthrie, G.D., Hsieh, P.A., Ryerson, T.B., Savas, O. & Shaffer, F. (2012) Review of flow rate estimates of the *Deepwater Horizon* oil spill. *Proceedings of the National Academy of Sciences*, 109 (50), 20260–20267. https://doi.org/10.1073/pnas.1112139108
Mertzlufft, D.W. (2021) *Pelagic Habitat Use by Benthic Fishes—Juvenile Scorpaenoids of the Oceanic Gulf of Mexico*. Master's Thesis, Nova Southeastern University, Fort Lauderdale, Florida, 64 pp.
Mito, S. & Uchida, K. (1958) On the egg development and hatched larvae of a scorpaenoid fish, *Pterois lunulata* Temminck et Schlegel. *Science Bulletin of the Faculty of Agriculture*, *Kyushu University*, 16 (3), 381–385.
Moser, H.G. (1996) Scorpaenidae: scorpionfishes and rockfishes. *In*: Moser, H.G. (Ed.), *The Early Stages of Fishes in the California Current Region*. *California Cooperative Oceanic Fisheries Investigations*, *Atlas No. 33*. Allen Press, Inc., Lawrence, Kansas, pp. 733–795.
Moser, H.G., Ahlstrom, E.H. & Sandknop, E.M. (1977) Guide to the identification of scorpionfish larvae (family Scorpaenidae) in the Eastern Pacific with comparative notes on species of *Sebastes* and *Helicolenus* from other oceans. *National Oceanic & Atmospheric Administration*, *National Marine Fisheries Service Technical Report*, *NMFS Circular*, 402, 1–71. https://doi.org/10.5962/bhl.title.62989
Mostowy, J., Malca, E., Rasmuson, L., Vásquez-Yeomans, L., Gerard, T., Sosa Cordero, E., Carrillo, L. & Lamkin, J.T. (2020) Early life ecology of the invasive lionfish (*Pterois* spp.) in the western Atlantic. *PLoS ONE*, 15 (12), e0243138. https://doi.org/10.1371/journal.pone.0243138
Motomura, H. & Matsuura, K. (Eds.) (2014) *Field Guide to Fishes of Yoron Island in the Middle of the Ryukyu Islands*, *Japan*. The Kagoshima University Museum, Kagoshima and the National Museum of Nature and Science, Tsukuba, 648 pp., 1808 figs.

Motomura, H., Béarez, P. & Romain, C. (2011) Review of Indo-Pacific specimens of the subfamily Scorpaeninae (Scorpaenidae), deposited in the Muséum national d'Histoire naturelle, Paris, with description of a new species of *Neomerinthe*. *Cybium*, 35 (1), 55–71.

Motomura, H., Causse, R. & Struthers, C.D. (2012) *Phenacoscorpius longilineatus*, a new species of deepwater scorpionfish from the Southwestern Pacific Ocean and the first records of *Phenacoscorpius adenensis* from the Pacific Ocean (Teleostei: Scorpaenidae). *Species Diversity*, 17 (2), 151–160.
https://doi.org/10.12782/sd.17.2.151

Motomura, H., Last, P.R. & Yearsley, G.K. (2007) Two new species of the scorpionfish genus *Trachyscorpia* (Sebastidae: Sebastolobinae) from the southern Indo-West Pacific, with comments on the distribution of *T. eschmeyeri*. *Zootaxa*, 1466 (1), 19–34.
https://doi.org/10.11646/zootaxa.1466.1.3

Moyer, J.T. & Zaiser, M.J. (1981) Social organization and spawning behavior of the pteroine fish *Dendrochirus zebra* at Miyake-jima, Japan. *Japanese Journal of Ichthyology*, 28 (1), 52–69.
https://doi.org/10.11369/jji1950.28.52

Nagasawa, T. & Kojima, J. (2014) Sebastidae. *In*: Okiyama, M. (Ed.), *An Atlas of the Early Stages of Fishes in Japan*. *Second Edition*. Tokai University Press, Hadano, pp. 585–606.

Papacostas, K.J., Carroll-Rielly, E.W., Georgian, S.E., Long, D.J., Princiotta, S.D., Quattrini, A.M., Reuter, K.E. & Freestone, A.L. (2017) Biological mechanisms of marine invasions. *Marine Ecology Progress Series*, 565, 251–268.
https://doi.org/10.3354/meps12001

Poss, S.G. & Eschmeyer, W.N. (2002) Scorpaenidae. *In*: Carpenter, K.E. (Ed.), *The Living Marine Resources of the Western Central Atlantic*: *FAO Species Identification Guide for Fishery Purposes*. *Vol. 2*. *Bony Fishes Part 1. Acipenseridae to Grammatidae*. Food and Agriculture Organization of the United Nations, Rome, pp. 1232–1265.

Resiere, D., Cerland, L., De Haro, L., Valentino, R., Criquet-Hayot, A., Chabartier, C., Kaidomar, S., Brouste, Y., Mégarbane, B. & Mehdaoui, H. (2016) Envenomation by the invasive *Pterois volitans* species (lionfish) in the French West Indies - a two-year prospective study in Martinique. *Clinical Toxicology*, 54 (4), 313–318.
https://doi.org/10.3109/15563650.2016.1143100

Richards, W.J. (2005a) Triglidae: searobins. *In*: Richards, W.J. (Ed.), *Early Stages of Atlantic Fishes*: *An Identification Guide for the Western Central North Atlantic*. *Vol. 1*. CRC Press, Boca Raton, Florida, pp. 1181–1184.

Richards, W.J. (2005b) Peristediidae: armored searobins. *In*: Richards, W.J. (Ed.), *Early Stages of Atlantic Fishes*: *An Identification Guide for the Western Central North Atlantic*. *Vol. 1*. CRC Press, Boca Raton, Florida, pp. 1185–1190.

Richards, W.J., Baldwin, C.C. & Röpke, A. (2005) Serranidae: sea basses. *In*: Richards, W.J. (Ed.), *Early Stages of Atlantic Fishes*: *An Identification Guide for the Western Central North Atlantic*. *Vol. 1*. CRC Press, Boca Raton, Florida, pp. 1225–1332.

Rüppell, E. (1838) Fische des rothen Meeres. *In*: Rüppell, E. (Ed.), *Neue Wirbelthiere zu der Fauna von Abyssinien gehörig*. Siegmund Schmerber, Frankfurt am Main, pp. 1–148.

Sabaj, M.H. (2020) Codes for natural history collections in Ichthyology and Herpetology. *Copeia*, 108 (3), 593–669.
https://doi.org/10.1643/ASIHCODONS2020

Sánchez, R.P. & Acha, E.M. (1988) Development and occurrence of embryos, larvae and juveniles of *Sebastes oculatus* with reference to two Southwest Atlantic scorpaenids: *Helicolenus dactylopterus lahillei* and *Pontinus rathbuni*. *Meeresforschung Reports on Marine Research*, 32 (2), 107–133.

Shadrin, A.M. & Emel'yanova, N.G. (2019) Embryonic and larval development and some reproductive-biology features of *Dendrochirus zebra* (Scorpaenidae). *Journal of Ichthyology*, 59 (1), 38–51.
https://doi.org/10.1134/S0032945219010156

Schultz, E.T. (1986) *Pterois volitans* and *Pterois miles*: two valid species. *Copeia*, 1986 (3), 686–690.
https://doi.org/10.2307/1444950

Smith, J.L.B. (1957) The fishes of the family Scorpaenidae in the western Indian Ocean. Part II.—The sub-families Pteroinae, Apistinae, Setarchinae and Sebastinae. *Ichthyological Bulletin*, *Rhodes University*, 5, 75–87, pls. 5–6.

Smith-Vaniz, W.F. & Collette, B.B. (2013) Fishes of Bermuda. *Aqua*, *International Journal of Ichthyology*, 19 (4), 165–186.

Sponaugle, S., Gleiber, M.R., Shulzitski, K. & Cowen, R.K. (2019) There's a new kid in town: lionfish invasion of the plankton. *Biological Invasions*, 21 (10), 3013–3018.
https://doi.org/10.1007/s10530-019-02070-1

Steindachner, F. (1900) Fische aus dem Stillen Ocean. Ergebnisse einer reise nach dem Pacific (Schauinsland, 1896–1897). *Anzeiger der Kaiserlichen Akademie der Wissenschaften*, *Mathematisch-Naturwissenschaftliche Classe*, 37 (1), 174–178.

Sutherland, W.J., Clout, M., Côté, I.M., Daszak, P., Depledge, M.H., Fellman, L., Fleishman, E., Garthwaite, R., Gibbons, D.W., De Lurio, J., Impey, A.J., Lickorish, F., Lindenmayer, D., Madgwick, J., Margerison, C., Maynard, T., Peck, L.S., Pretty, J., Prior, S., Redford, K.H., Scharlemann, J.P.W., Spalding, M. & Watkinson, A.R. (2010) A horizon scan of global conservation issues for 2010. *Trends in Ecology & Evolution*, 25 (1), 1–7.
https://doi.org/10.1016/j.tree.2009.10.003

Temminck, C.J. & Schlegel, H. (1843) Pisces. *In*: de Siebold, P.F. (Ed.), *Fauna Japonica*, *sive descriptio animalium, quae in itinere per Japoniam*, *jussu et auspiciis, superiorum, qui summum in India Batava imperium tenent, suscepto, annis* 1823–1830 *collegit, notis, observationibus et adumbrationibus illustravit Ph. Fr. de Siebold*. *Parts 2–4*. Apud Arnz et

Socios, Leiden, pp. 21–72.
https://doi.org/10.5962/bhl.title.124951
van der Laan, R., Fricke, R. & Eschmeyer, W.N. (Eds.) (2023) Eschmeyer's Catalog of Fishes: Classification. Available from: https://www.calacademy.org/scientists/catalog-of-fishes-classification/ (accessed 1 July 2023)
Vásquez-Yeomans, L., Carrillo, L., Morales, S., Malca, E., Morris, J.A., Jr., Schultz, T. & Lamkin, J.T. (2011) First larval record of *Pterois volitans* (Pisces: Scorpaenidae) collected from the ichthyoplankton in the Atlantic. *Biological Invasions*, 13 (12), 2635–2640.
https://doi.org/10.1007/s10530-011-9968-z
Victor, B.C. & Ianniello, L. (2020) *Prionotus murielae* Mowbray, 1928 is the juvenile of the bandtail searobin *Prionotus ophryas* (Teleostei: Scorpaeniformes: Triglidae). *Journal of the Ocean Science Foundation*, 35, 76–85.
https://doi.org/10.5281/zenodo.3962673
Weigle, S.M., Smith, L.D., Carlton, J.T. & Pederson, J. (2005) Assessing the risk of introducing exotic species via the live marine species trade. *Conservation Biology*, 19 (1), 213–223.
https://doi.org/10.1111/j.1523-1739.2005.00412.x
Whitaker, J.M. & Janosik, A.M. (2020) Missing the mark(er): pseudogenes identified through whole mitochondrial genome sequencing provide new insight into invasive lionfish genetics. *Conservation Genetics*, 21 (3), 467–480.
https://doi.org/10.1007/s10592-020-01263-9
Wilcox, C.L., Motomura, H., Matsunuma, M. & Bowen, B.W. (2018) Phylogeography of lionfishes (*Pterois*) indicate taxonomic over splitting and hybrid origin of the invasive *Pterois volitans*. *Journal of Heredity*, 109 (2), 162–175.
https://doi.org/10.1093/jhered/esx056
Williams, S.L., Crafton, R.E., Fontana, R.E., Grosholz, E., Ha, G., Pasari, J.R. & Zabin, C.J. (2015) A vector analysis of marine ornamental species in California. *Management of Biological Invasions*, 6 (1), 13–29.
https://doi.org/10.3391/mbi.2015.6.1.02
Yoshida, T., Motomura, H., Musikasinthorn, P. & Matsuura, K. (Eds.) (2013) *Fishes of Northern Gulf of Thailand*. National Museum of Nature & Science, Tsukuba, Research Institute for Humanity & Nature, Kyoto, and Kagoshima University Museum, Kagoshima, 239 pp.

Appendix

TABLE 1. Collection information for larvae of *Dendrochirus barberi* and the juvenile *D. hemprichi* examined in this study and archived at the Los Angeles County Museum of Natural History (LACM).

Taxon	Count	mm SL	Museum record	Collection date	Location collected	Collector
Dendrochirus barberi	10	8.6–9.2; 11.2–14.5	LACM 45868.010	March 3, 1979	O'ahu, Hawai'i	T. A. Clarke
Dendrochirus barberi	1	10.2	LACM 45962.003	June 4, 1978	O'ahu, Hawai'i	T. A. Clarke
Dendrochirus barberi	1	10.4	LACM 45967.009	July 3, 1978	O'ahu, Hawai'i	T. A. Clarke
Dendrochirus hemprichi	1	21.0	LACM 31619.017	December 5, 1970	South Sail Rock Channel, Kenya	P. Saw